PACS numbers:

Copper−Titanium Solid Solutions are New Generation of High Strength Age-Hardening Alloys

K. V. Chuistov

G. V. Kurdyumov Institute for Metal Physics, N. A. S. of the Ukraine,
36 Academician Vernadsky Blvd.,
UA-03680 Kyyiv-142, STM, Ukraine

In this review the precipitation phenomenon and age-hardening response in Cu−Ti alloys founded on the Ukrainian and Russian authors investigations mainly was discussed. At that point, it was especially underlined that a mechanism of the early stage of the decomposition was not as spinodal one (American authors point of view) but more likely as a nucleation of fine-scale coherent precipitates of the metastable α'-phase (Cu_4Ti). The kinetics of the continuous and discontinuous (cellular) precipitation; the morphology of the metastable α'-phase and stable β-phase precipitation; an influence of the external effects (plastic and ultrasonic deformation, external pressure, radioactive irradiation) on these processes; the nature of the high age-hardening response in Cu−Ti alloys and the reversion phenomenon was considered. It was postulated that these alloys could replace the beryllium bronze successfully according to their mechanical properties.

Виконано огляд оригінальних досліджень українських та російських авторів, які відносяться до вивчення явища виділення і зміцнення при старінні Cu−Ti сплавів. При цьому особливо підкреслено, що механізм навчальних стадій розпаду не є спінодальним (точка зору американських авторів), а скоріше являє собою зародкування дисперсних частинок когерентної метастабільної α'-фази (Cu_4Ti). В огляді також розгляниті закономірності кінетикі, морфології неперервного та преривчатого (коміркового) розпаду, морфологія виділення метастабільної α'- і стабільної β-фаз; вплив зовнішних чиників (пластичної та ультрозвукової деформації, зовнішнього тиску, радіоактивного опромінювання) на ці процеси; можливі механізми надзвичайного зміцнення старіючих Cu−Ti сплавів та явище звороту міцності. Зроблено висновок, що по своїх механічних властовостях ці сплави можуть з успіхом замінити берильову бронзу.

Проведен обзор результатов процессов старения Cu−Ti сплавов, сопрово-

ждающихся их необычно высоким упрочнением, основанной в основном на исследованиях украинских и российских авторов. При этом особо подчеркнута малая вероятность спинодального механизма в этих сплавах (точка зрения американских авторов). Полученные экспериментальные данные указывают на большую вероятность зародышеобразования дисперсных зародышей метастабильной когерентной α'-фазы (Cu_4Ti). В обзоре рассмотрена кинетика и морфология непрерывного и прерывистого (ячеистого) выделения метастабильной α'- и стабильной β-фаз; влияние внешних воздействий (пластической и ультразвуковой деформации, внешнего давления и радиоактивного облучения) на эти процессы; возможные механизмы высокого упрочнения состаренных $Cu-Ti$ сплавов и явление возврата твердости. Сделан вывод, что по своим механическим свойствам эти сплавы вполне могут заменить бериллиевую бронзу.

1. Introduction

It is well known that since the 20-th years of the XX century the age-hardened alloys have been found a wide application in various kind of the human business. For example, they are needed for manufacturing the various engineering materials, particularly aluminum for aircraft industry, hard magnets, refractory materials etc. Here we would like to make the accent on age-hardened alloys with both high elastic and electrical conductivity properties. At the present time the champion among these alloys is the beryllium bronze [1]. This material has very high strength properties after aging (U.T.S. = 1300−1500 MPa; Y.S. = 1000−1100 MPa; E.L. = 900−1000 MPa but $\delta = 1-3\%$). Along with that it possesses good electrical conductivity properties ($1/\rho = 12.5 \cdot 10^{-4}$ $Om^{-1}cm^{-1}$) that makes the beryllium bronze as large-scale product for the springs, elastic conducting contacts, elastic diaphragms and others elastic elements manufacturing. In spite of these unique mechanical properties this material has a very big shortcoming — it production connects with large ecological danger since the gasiform beryllium oxide formed at that is very toxic. Moreover, the beryllium bronze is very sensitive to the heat treatment regimes, a deviation from that leads often to the spoilage. Along with that, the utilizing temperature of Cu−Be has not to exceed 150°C since higher it the creep process takes place.

The all this forces to sick new high strength materials with good electrical conductivity. Such materials could be copper−titanium alloys with high age-hardening response [2]. The age hardening of

these alloys containing 1–5 wt.% Ti has been known since the 1930s [3–5]. Then Cu–Ti alloys have kept an eye of researchers in 1950s [6]. But the main interest to these alloys has emerged when independently one after another the satellite reflections (sidebands) flanked the Brag's ones on the powder X-rays films were reported in our short communication [7] and in the letters to the editor by Jack Manenc [8]. After that two corresponding papers were published in 1960 [9, 10]. For an explanation this phenomenon these authors used Daniel's and Lipson's model [11] where the satellite appearance have been accounted for the periodical (sinusoidal) distribution of an alloying element concentration in the one of the crystal direction. On other words, this model described the periodical distribution of coherent precipitations in this crystal direction. It was called as 'modulated structure' (m.s.) [11]. Whereupon, the more realistic models were treated since it turned out that the satellites had different intensity or different position with respect to Bragg's reflexes on the X-rays films [12–17]. Some of these models [12, 13] have used Guinier's one-dimensional complex [18] or three-dimensional complexes for explanation these pictures [15, 16]. The competence of these models application was based on a ground that in some age-hardening alloys (Co–Ti [17], Co–Cu [18]) the satellites appearance did not correspond to the periodical precipitates distribution and such regular morphology was created during particles growth only.

An important breakthrough in the understanding the precipitation reaction in Cu–Ti super saturated solid solutions during aging occurred when in works [10, 21–24] the formation of the metastable intermediate $\alpha'(\beta')$-phase was established. At first it was concluded that α'-phase had f.c.t. lattice with the constants $a = 0,369$ nm; $c = 0.362$ nm [10, 21, 22]. But in subsequent works [23, 24] it was claimed that its structure was similar to $D1_a$ (b.c.t.) superstructure with the composition Cu_4Ti.

The main task of this review article is to acquaint the readers, the foreigner especially, with the results of the age-hardening Cu–Ti alloys investigations obtained by Russian and Ukrainian authors.

2. The Mechanisms of Decomposition in Cu–Ti Alloys

According to recent version of the Cu–Ti phase diagram (Fig. 1) [25] the terminal f.c.c. Cu-rich solid solution (α) is in equilibrium with $\beta(Cu_3Ti$ or $Cu_4Ti)$-phase with orthorhombic lattice (space group Pnma) [26, 27].

Moreover, it was found that in the β-phase the polymorphic transformation might be realized [27] (Fig. 2). At the same time, the coherent α'-phase solvus curve was constructed in Cu-rich part of the Cu–Ti phase diagram [25] (Fig. 3).
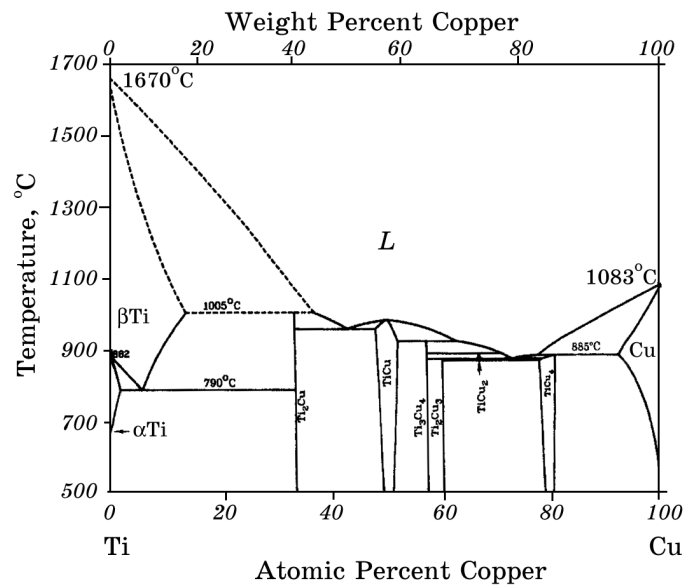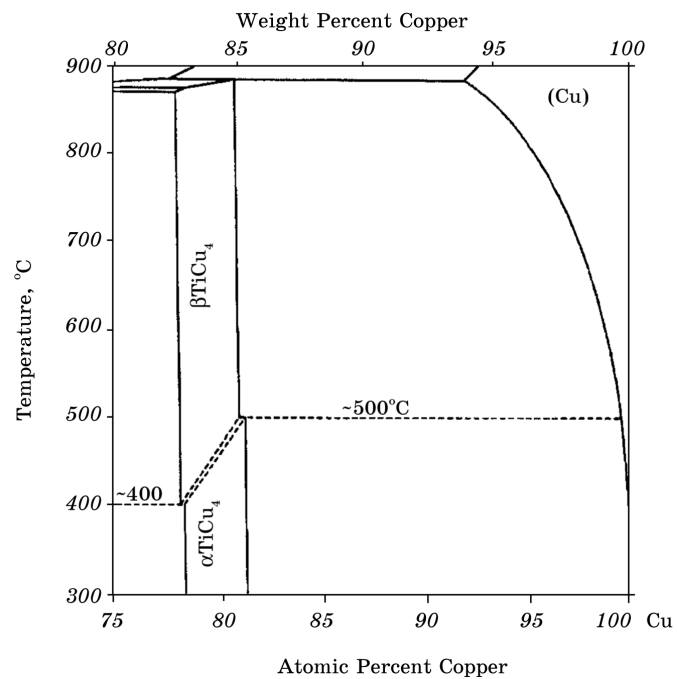
Fig. 1. The Cu–Ti equilibrium phase diagram [27].

Fig. 2. The Cu-rich portion of Cu–Ti diagram showing the polymorphic transformation in Cu$_4$Ti phase [27].
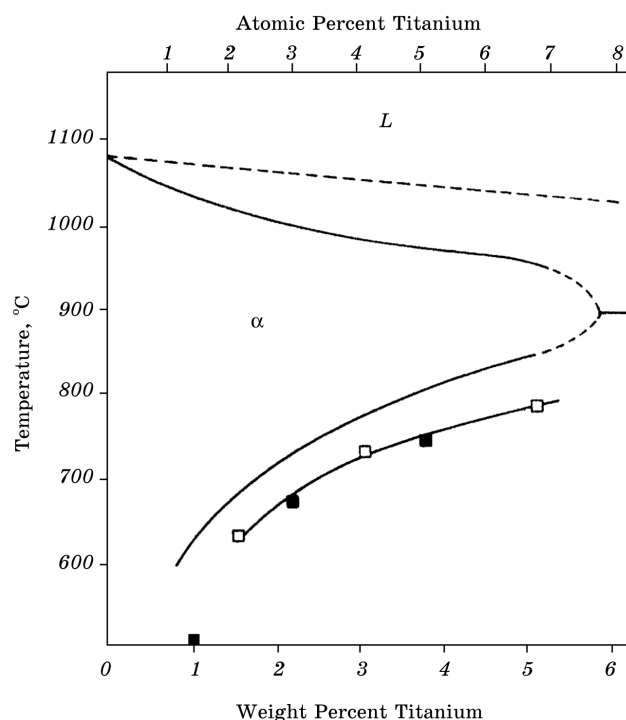
Fig. 3. The measured metastable α' ($D1_a$) coherent solvus curve in Cu-rich region [25].

At the beginning of Cu–Ti alloys investigations most studies have utilized X-ray diffraction methods being analyzed diffuse scattering [7–10, 13–18]. According to these data the precipitation sequence in this system was presented as: s.s.s. → m.s. → metastable Cu_4Ti $\alpha'(\beta')$-phase → stable Cu_3Ti β-phase precipitation.

Here s.s.s. — terminal super saturated solid solution Ti in Cu; m.s. — modulated structure: periodical distribution of the solute-lean and solute riche regions in [100] crystal direction. It should be remarked that X-ray analysis did not show any diffuse scattering near the matrix reflexes in the quenched state of the Cu–Ti alloys with 3–5 wt.% Ti [7–10]. Only after aging these alloys at the temperatures 300–500°C the additional diffuse maxima — satellites flanked the main reflexes could be observed. At the same time, it is necessary to underline the following peculiarity. As a rule, the 'satellite' stage of the decomposition of Cu–Ti alloys was character-ized by narrow matrix reflexes and by invariable of the average parameter a of its lattice [7–9]. This result may indicate that 'true precipitation' does not occur and the 'satellite' stage corresponds to the formation of some concentration heterogeneities — periodical

concentration waves or zones (complexes) that does not create the elastic strains in a matrix. As it will be discussed later, TEM analysis showed that these heterogeneities *represent the individual zones (complexes) distributed arbitrary in a matrix rather than continuous concentration waves*. This complexes have particular interior construction [15, 16] and largely coherent with a matrix. Probably their composition is close to a matrix and the presence the satellites flanked the matrix reflexes may speak both about *structural and optical coherence*.

Undoubtedly, the utilizing of the transmission electron microscopy (TEM) in the precipitation studying in Cu−Ti alloys has enabled to define the details of this phase transformation more exactly [28−33]. In the early investigations [28−30] it has been found that the quenched state of the Cu−Ti alloys with 4−5 wt.% Ti had been heterogeneous. In this case these heterogeneities have had the equiaxial shape, the middle size about 6−8 nm and arbitrary distributed in a matrix. In this point, only sick satellites were observed in the electron selected area diffraction pattern. Such precipitation morphology did not change after aging at 300°C, 1 h (Fig. 4). At that, the middle size of the heterogeneities was ~8−10 nm [29]. In Fig. 4 the dark-field image of such structure is represented too. It got in the matrix reflexes for receiving more correct picture of these heterogeneities since its superstructure reflexes were almost invisible. These results allowed to suppose that these heterogeneities might be described by Guinier's complex but only in three-dimensional mode [15, 28, 29].
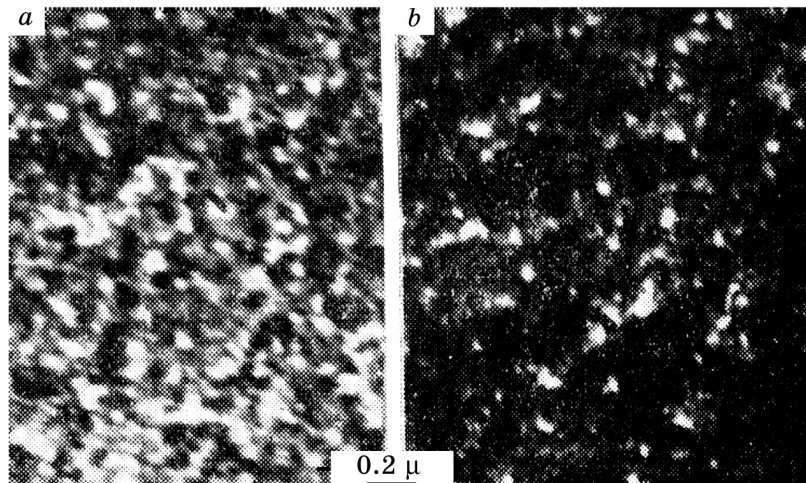

Fig. 4. An electron microstructure of Cu−5 wt.% Ti alloy aged at 300°C, 1 h: *a* — bright field; *b* — dark field in the 220 matrix reflex [29].
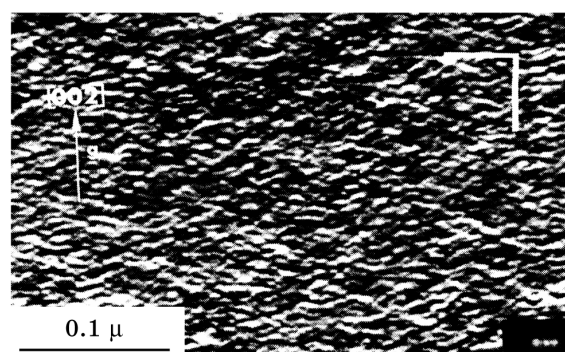
Fig. 5. Periodic strain contrast along (200) matrix direction corresponding to quenched microstructure of Cu–4 wt.% Ti [33].

On the other hand, in [31–33] the quite different TEM contrast was observed in the quenched state of Cu–Ti alloys almost the same composition as early as (Fig. 5).

The authors of the work [33] concluded that this micrograph clearly indicated on clustering during the Cu–Ti quench giving rise to matrix strain contrast striations along the traces of the {100} matrix planes.

In accordance with [34], this picture corresponds to three-dimensional macro-lattice composing the coherent Cu_4Ti phase particles. The presence of that contrast initiated the authors [2, 24, 33] to conclude the spinodal decomposition mode during quenching of the Cu–Ti alloys containing more 1 wt.% Ti. At that, very week superstructure reflexes of that phase were found in the quenched state [33]. Incidentally, this observation does not look in favor of this mechanism of the early stage of the decomposition since Cahn's theory of the spinodal transformation postulates in this case concentration waves presence that are small in the amplitude and are large in the length. More attractive mechanism of the early stage of Cu–Ti alloys aging is the concentration heterogeneities — nucleuses of the coherent Cu_4Ti phase formation during quenching as in the case of Ni base alloys [35]. For example, the presence of the precipitates contrary to concentration waves was indicated in such 'spinodal' alloys as Cu–Ni–Fe ones [36]. However, the different morphology of Cu_4Ti phase precipitation (non-periodical [28–30] and periodical [33]) experimentally observed in the quenched Cu–Ti alloys with 3–5 wt.% Ti does not understand completely. Perhaps it may be explained by various conditions of the alloys producing and quenching. Moreover, until now don't appear any HREM results that could indicate on the singular ordering in the terminal solid solution of the Ti in the Cu as in the case of the Al–Li alloys, for example [37].

Hence, we hold the opinion that *the mechanism of the early stage of the decomposition in Cu–Ti alloys consists in the precipitation of the ordered coherent Cu$_4$Ti phase during quenching of Cu–Ti alloys that occurred by way of concentrated three-dimensional complexes formation as nucleuses of the intermediate metastable Cu$_4$Ti phase.* As regards of the terminal Cu–Ti solid solution it is possible it contents short-range ordered regions $D1_a$ kind in the high-temperature single phase field [38]. Next, these regions may serve as the places for the nucleation of the complexes and then Cu$_4$Ti metastable phase.

Thus, continuous decomposition in the super saturated Cu–Ti solid solutions may be described as s.s.s. → concentration complexes → ordered coherent Cu$_4$Ti (a.d.) → ordered coherent Cu$_4$Ti (m.s.). Here s.s.s. — super saturated Cu–Ti solid solutions; a.d. — arbitrary distributed particles; m.s. — modulated structure. This sequence takes into account that *m.s. forms due to elastic interaction between coherent particles during their growth for the coalescence but not due to spinodal decomposition.*

The crystalline structure of the Cu$_4$Ti metastable α'-phase has been determined at first as f.c.t structure with the constants: $a = 0.369$ nm, $c = 0.362$ nm [10, 21, 22]. It is need to notice that in [21] the crystalline structure of this phase and its lattice constants were determined in electrolytic extracted particles. After that in [23] the structure of Cu$_4$Ti phase was described as b.c.t. superstructure ($D1_a$) with the lattice constant $a = 0.584$ nm; $c = 0.362$ nm. It is known that this superstructure is a crystallographic derivative of the parent f.c.c. matrix in that the ordered structure can form continuously by rearrangement of Cu and Ti atoms on the sites of the terminal f.c.c. lattice (Fig. 6).
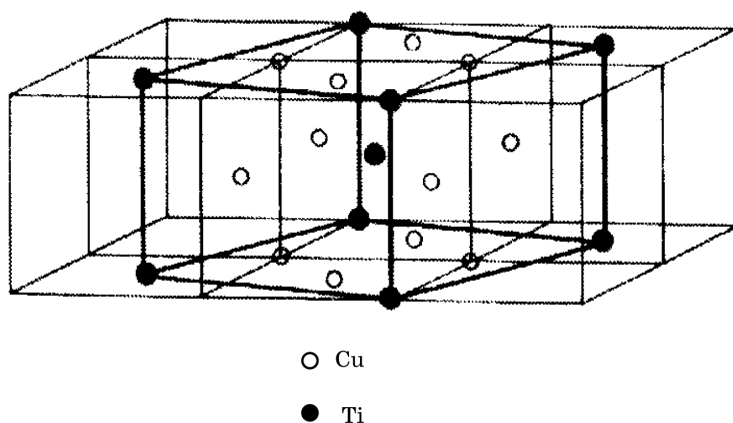

O Cu

● Ti

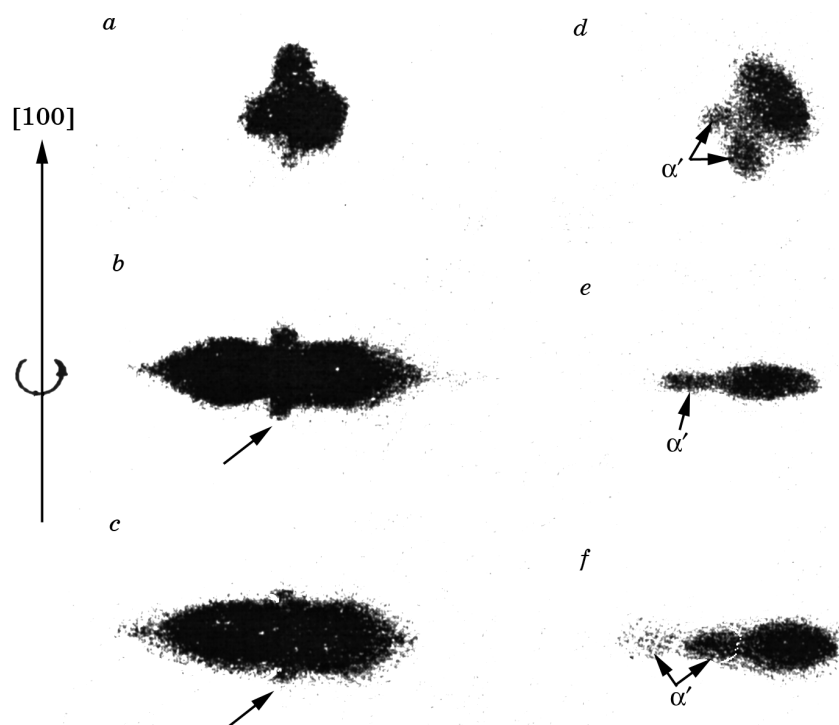**Fig. 6.** Schematic of the $D1_a$ superlattice phase Cu$_4$Ti as a derivative of the f.c.c matrix [33].

Fig. 7. The fragments of the X-ray swinging film of the micro-single crystal of the Cu–5 at.% Ti alloy aged at the temperatures: 400°C, 8 h — a–c; 500°C, 8 h — d–f; reflexes: 111 — a, d; 200 — b, e; 220 — c, d. Cuk_{α} — radiation [39].

The possible distortions being created during α'-phase precipitation was analyzed by X-ray study using swinging micro-single crystal method [39]. The Fig. 7 shows the main results obtained in this work. From this picture it is seen that along with the satellites observing in the alloys with the modulated structure [40] an additional diffuse scattering are presented and showed by arrows. At that, they look like short streaks and tilt to the axis of the specimen swinging [001]. After an aging temperature increasing up to 500°C this diffuse scattering transformed to two sharply reflexes from the α'-phase (Fig. 7, d–f). So, two azimutally distributed reflexes from α'-phase near the $(111)_{\alpha}$ spot are present (Fig. 7, d), whereas, near $(220)_{\alpha}$ they look like the tetragonal doublet (Fig. 7, e, f). At the same time, in [39] the series of the X-ray films were obtained for a stationary single crystal rotated through 18′ around [001] axis. The diffuse scattering cross-sections and their schematic representation near the reciprocal lattice (RL) node 200 are depicted in Fig. 8. The numerical treatment of this picture shows that the direction of dif-
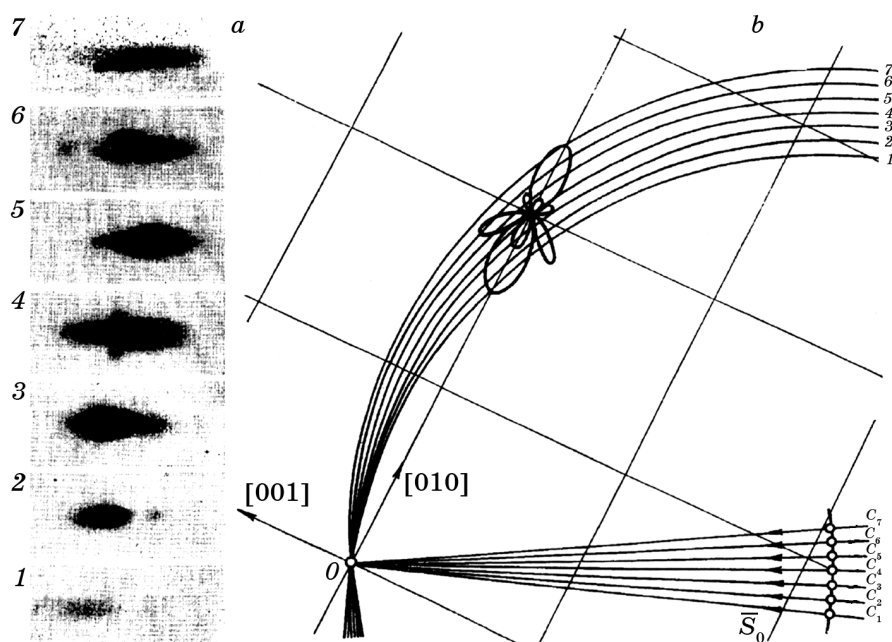
Fig. 8. *a* — the set of the diffuse scattering cross-sections near the 200 reflex of the Cu–5 at.% Ti alloy aged at 400°C, 8 h after rotating of the stationary single crystal on 18′. The Cuk_α — radiation. Magnification ×10. *b* — the corresponding cross-sections of the diffuse scattering regions in the reciprocal space near the node 200 [39].
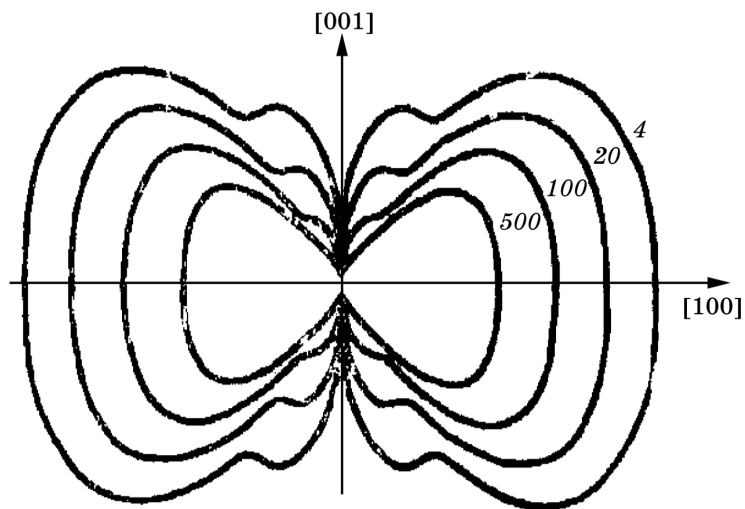

Fig. 9. Isodiffuse curves in the place (100) near the node (h00) of the RL. The case of the Cu elastic constants. The intensities are marked in the relative units [39].

fuse streaks in the RL is $\langle 110 \rangle$. For explanation of these effects the analysis of the diffuse scattering by the tetragonal precipitate into the elastically anisotropy matrix was fulfilled [39]. It was based on the following equation [41].

$$I_D = \alpha \left| \bar{f} \mathbf{q}_1 \mathbf{A}_\mathbf{q} C_\mathbf{q} \right|^2, \tag{1}$$

where α is a constant; $\bar{f}$ is an average structural amplitude; $\mathbf{q}_1$ is a diffraction vector, $\mathbf{q}_1 = \mathbf{q} + 2\pi\mathbf{H}_n$, $\mathbf{H}_n = $ RL vector the nearest to end of the vector $\mathbf{q}_1 = 2\pi$; $\mathbf{A}_\mathbf{q}$ is an amplitude of the static distortion waves and $C_\mathbf{q}$—a Fourier component of the concentration distribution. In this case $C_\mathbf{q}$ was determined from the equation

$$\delta c(\mathbf{r}) = C_m \exp(-\beta \mathbf{r}^2).$$

Here δc is a deviation of the concentration in the enriched region from the average in the matrix — c_0. In the Equation 1 the scattering due to the difference of the diverse scattering factors of Cu and Ti did not take into account.

The lattice constant of Cu_4Ti phase along c axis was observed to be closed to the matrix constant a since near the reflex $(200)_m$ there was a single reflex of this phase but near the $(220)_m$ two precipitate reflexes were observed (Fig. 7, e and f) [39]. At the same time, it was shown that for $D1_a$ superstructure (Ni_4Mo — type) six variants might be realized (Fig. 6) [33]:

$$[001]_{ppt} \parallel [001]_m; \quad [100]_{ppt} \parallel [3\bar{1}0]_m.$$

From the angle position of the reflexes near the $(220)_m$ of α'-phase electrolytical extracted particle, the tetragonal ratio $c/a = 0.98$ was estimated [21]. The crystal structure of the equilibrium β-phase (Cu_3Ti) may be described as orthorhombic lattice with the constants $a = 0.2585$ nm; $b = 0.4527$ nm; $c = 0.4351$ nm, or as hexagonal structure with the constants $a = 0.261$ nm; $c = 0.427$ nm in accordance with [42]. The orientation relationship of the β-phase and the matrix is $\{0001\}_\beta \parallel \{111\}_m$; $\langle 2\bar{1}\bar{1}0 \rangle_\beta \parallel \langle 110 \rangle_m$ [42]. At the same time, in [27] it was postulated that β-phase had the composition Cu_4Ti and has undergone the polymorphic transformation (Fig. 2, a). The nucleation mechanisms of β-phase is heterogeneous, as rule, but it may originate from intermediate α'-phase during aging or plastic deformation that will be discussed later.

3. The Morphology of the Precipitation

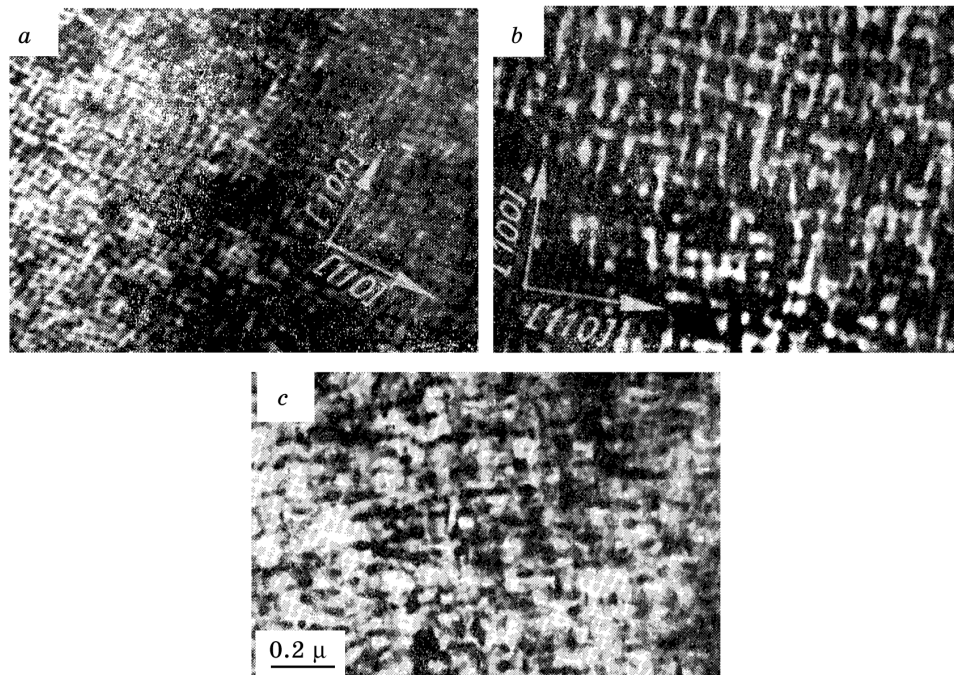Just the onset of the investigation of the Cu–Ti age-hardened alloys

Fig. 10. The mode of the distribution of the metastable tetragonal α'(Cu_4Ti)-phase in an alloy Cu–5.5 wt.% Ti after aging: a — for 30 min at 450°C; b — for 1 h at 500°C; c — for 3 h at 500°C. Bright — field [29].

it was supposed that the morphology of the early stage of the decomposition was quasi-regular that was concerned with the modulated structure formation [43]. Moreover, it was noticed that this structure detected in the quenched Cu–4 wt.% Ti alloy in an alloy with 1 wt.% Ti it did not observe [2, 32, 33]. However, as it was described above (Fig. 4) both in the quenched state and at early stage of the decomposition of Cu–(3–5) wt.% Ti the uniformly distributed equiaxed particles was found. Fig. 10 is an example of that distribution. As seen from these pictures at the beginning of Cu–Ti alloys aging α'-phase particles organize the quasi-regular net or rather the net composed of the domains containing some regular distributed particles. At the same time, the particles inside the domains are arranged along the directions $\langle 100 \rangle$. It is interesting to notice that such peculiarity of the modulated structure has been underlined in aged alloy Fe–Be [44]. In this case the modulated structure may be represented as three-dimensional 'macro-lattice' of nodes occupied by coherent particles. Along with that, this configuration consists from tetragonal domains. Now it is well known that in most cases the modulated structure formation cause by an elastic interaction between

the coherent precipitates in the elastically anisotropy matrix [45]. At that, the particles arrange along soft modulus directions that depends on the sign of the anisotropy factor $\xi = C_{11} - C_{12} - 2C_{44}/C_{44}$, where C_{ik} — are the elastic constants [45]. The subsequent division of the 'macro-lattice' on tetragonal domains was explained by the further decreasing of the elastic energy of the heterogeneous system composing the elastic interaction particles [44].

An increasing of the aging temperature up to 500°C of Cu—Ti alloys leaded to rows of rod-like particles formation being elongated along $\langle 100 \rangle$ directions (Fig. 10, b). Such phenomenon may be explained by near interaction between the particles during coalescence in these rows [40]. The same type of the modulated structure — periodic arrays of block-like rods of the coherent $\alpha'(\beta')$-phase aligned along $\langle 100 \rangle$ matrix directions. was observed in [28] and some later in [33]. During increasing an aging duration to 3 h at 500°C the shape of rod-like $\alpha'(\beta')$-phase particles was distorted although the tendency to their arrangement along $\langle 100 \rangle$ direction remained (Fig. 10, c).

Perhaps this may be explained by the complex character of the coalescence of the elastic interacted precipitations constituted the modulated structure [46, 47]. So, in this case not only the particles size growth but the transformation inside of the domain itself took place [47]. After annealing of Cu—5.5 wt.% Ti alloy at 600°C three types of the precipitates were observed: elongated plate-like particles situated along $\langle 100 \rangle$ inside of the grain volume, precipitates in Widmanstätten form oriented along $\langle 111 \rangle$ (Fig. 11, a) and particles discontinuous precipitated on the grain boundaries (Fig. 11, b). The all these precipitates belonged to the stable $\beta(Cu_3Ti)$-phase that non-isomorphic and incoherent to matrix. The Widmanstätten precipi-

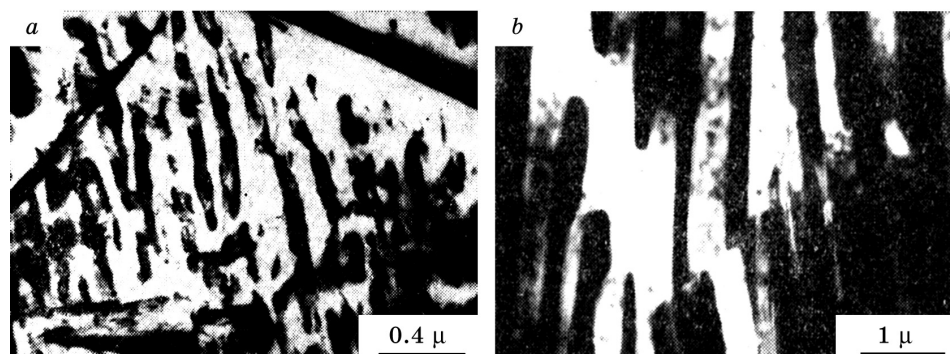**Fig. 11.** The stable β-phase precipitation: a — in the Widmaschtett's form (indicated by arrows): b — as cell decomposition. The Cu—5.5 wt.% Ti alloy aged for 1 h at 600°C. Bright — field [29].

tates had the {111} habit planes. The same results have been discussed in [30] where the discontinuous precipitation of the β-phase it was called as recrystallization reaction.

4. The Kinetics of the Precipitation in Cu–Ti Alloys

Since the rate of the initial products formation in Cu–Ti decomposing alloys is very high and occurs during quenching the kinetics of this stage of aging did not investigate yet. This situation is typical for the most aging 'satellites' alloys [43]. Usually the kinetics of the continuous precipitation is studied during aging of the quenched alloys. As to Cu–Ti alloys in [9, 48, 49] the kinetics of the early stage of the decomposition was studied by X-ray and resistivity methods (Fig. 12). As seen from Fig. 12 the kinetics curves of the electrical resistance change at various temperatures have usual relaxation mode. At the same time, the early stage of transformation are characterized by the big rate of changing and this rate rises with the temperature. An absent of the incubation period and the big rate of the precipitation on the onset of this process correspond to the aging with the very small activation energy of the nucleation that is typical for the isomorphous phase formation. It well known that the kinetics of the phase transformation may be described in general by the equation [50]

$$x = 1 - \exp\left(-\frac{t}{\tau}\right)^n.$$ (2)

Here x is the value of the transformation volume and an exponent n depends on the shape of the precipitate, for example, for plate-like particle $n = 0.5$. Supposing that $x = \Delta\rho_t/\Delta\rho_\infty$, where $\Delta\rho_t$ is a change of the resistivity for an aging time t and $\Delta\rho_\infty$ is the corresponding change when the ρ becomes the constant. Taking this into account, the curves in Fig. 12 were reconstructed on the base of the equation (2) (Fig. 13). It may be notice that the results of Fig. 12 and 13 correspond to two intervals of transformation: the first interval agrees with the free growth of the particles ($n = 0.15$) and the second one — with their coalescence ($n = 0.25$). However, as has been mentioned higher in the alloy with the modulated structure the coalescence occurred by more complex mechanisms than in a usual kind of this process. Therefore, these data need to regard as approximate ones. On the other hand, in [31] it was shown that a law of the enlargement of the average wavelength of modulated spacing (Cu$_4$Ti phase particles) vs (aging time)$^{1/3}$ often corresponds to

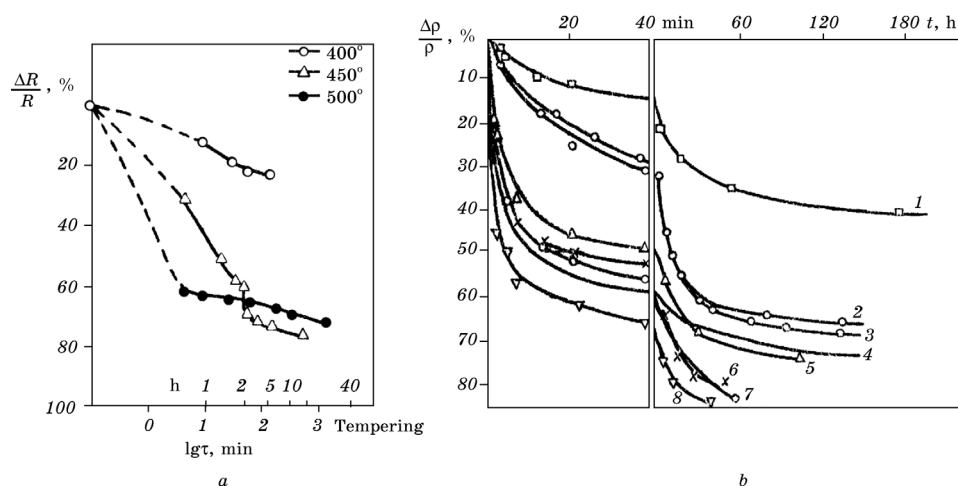**Fig. 12.** The kinetics of the resistivity change of Cu–Ti alloys: *a* — with 4.45 wt.% Ti [9]; *b* — 4.7 wt.% Ti aged at temperatures: *1* — 340; *2* — 400; *3* — ε = 50% + 400; *4* — 500; *5* — 450; *6* — ε = 12% + 500; *7* — ε = 50% + 450; *8* — ε = 50% + 500 (°C) [48].
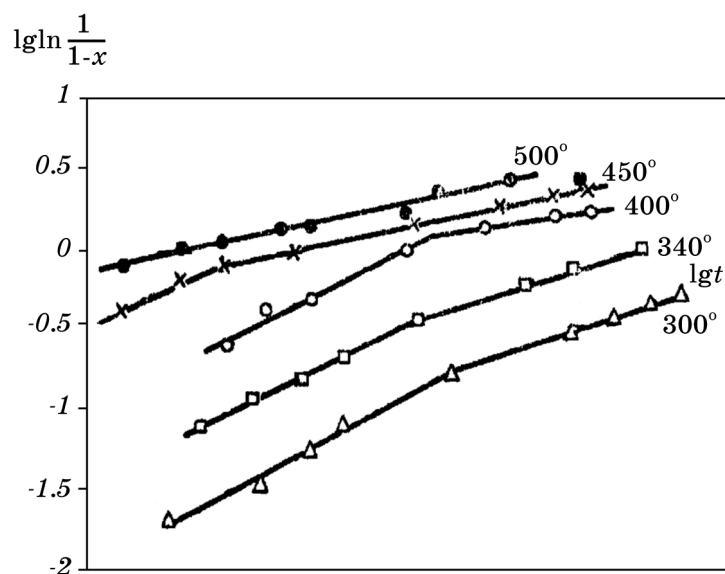

Fig. 13. The temporal dependence of $\lg\ln 1/(1-x)$ for the alloy Cu–4.7 wt.% Ti at various temperatures [48].

Lifshits–Slyozov' theory of a coalescence [51]. By the way, this takes place for many Ni-base alloys too [40]. Consequently, for the aging alloys with the modulated structure where the elastic coherent stresses not so large the law $r \sim t^{1/3}$ may be correct.

However, it is rather surprising that the coarsening of the modulated structures with a large degree of interconnectivity under mutual influence of surface and elastic strain energy should obey essentially the same kinetic law. Although Cahn shown the correctness of this law for the later stages of the spinodal decomposition this result is not well understood.

The value τ in (2) determines the temperature dependence of the aging rate [50]

$$\tau = A \exp\left(\frac{Q}{RT} \right), \qquad (3)$$

where A is a constant and Q is an activation energy. Constructing a graph of the dependence $\ln t_i - 1/T_i$ (Fig. 14) the activation energy of
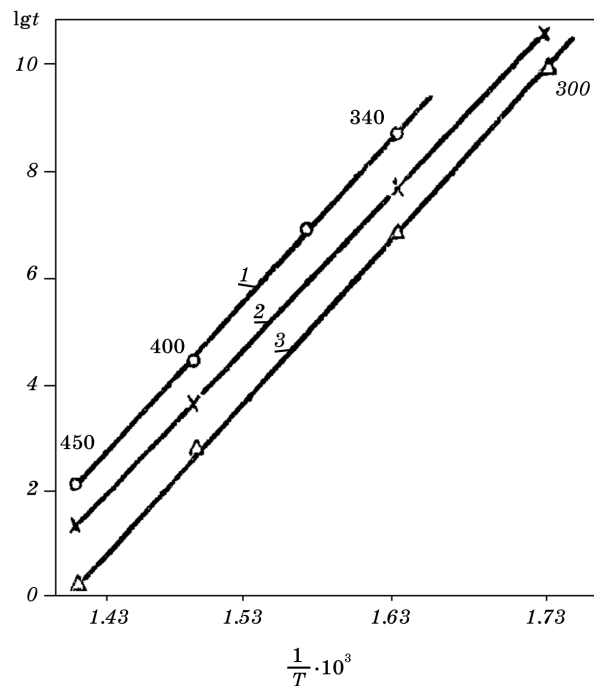

Fig. 14. An aging time dependence on the reciprocal temperature for the decreasing of the ρ to the values: *1* — 20; *2* — 30; *3* — 40% [48].

the process may be determined on the slope angle. The presence of the parallel curves in Fig. 14 speaks about the common process controlling an aging up to the onset of the discontinuous precipitation. The activation energy calculated from this picture was 43 ± 3 kcal/mole that close to activation energy of the volume diffusion Ti in Cu [48]. Afterwards, this value measured from the equation $r \sim t^{1/3}$ was equal $51,2 \pm 9,5$ kcal/mole [33] that in general was close to the first one.

It was found that after aging of Cu–Ti alloys at $T > 450°C$ the equilibrium β-phase precipitated by the discontinuous mode [22, 52]. At that, it well known that this mode of precipitation mainly is controlled by surface diffusion if a relation $D_b/D_v > d/\lambda$ [40].

Here D_b, D_v are coefficients of a boundary and volume diffusion correspondently; d is a distance between lamellas of the β-phase in the cell and λ is the width of the cell boundary. Using an equation (2) in [48] it was found that an exponent $n = 2$ that corresponded to the discontinuous decomposition [53]. Moreover, the relation between the values $\lg \ln 1/(1-x)$ in the dependence on aging duration ($\lg t$) was not only linear but for various values x was parallel. The activation energy of this process calculated from the inclination angle was equal $Q_a = 20$ kcal/mole that was less than for volume diffusion and probably corresponds to the boundary one [52].

The kinetics of the discontinuous precipitation in Cu–Ti alloys was investigated more detail by O. Smatko and M. Itkin in the wide temperature range [54–57]. For this purpose an alloy Cu–4.35 wt.% Ti was studied at the temperature interval 600–700°C [54] where discontinuous precipitation occurred predominantly [58]. Using the quantitative metallography the temporal dependence of the cells formation rate ($\dot{N}$) for different temperatures was obtained (Fig. 15). As depicted in Fig. 15 it is non-monotone: at the beginning of the transformation the value increases rapidly then culminates and whereupon quickly goes down. It was found that these results were in good accordance with Cahn's theory for grain boundary nucleation [59].

The other interesting result concerned the diffusion mode depending on aging temperatures [57]. It turned out that at 550–650°C in the Cu–5.7 at.% Ti alloy the volume diffusion plays the definite role in the discontinuous precipitation, at that point, in this case an activation energy of the volume diffusion $Q_v = 57.24$ kcal/mole. Conversely, at temperatures 450–500°C the boundary diffusion endows with $Q_b = 26.94$ kcal/mole. It is interesting that the same situation was observed for cellular precipitation in Co–Ta and Ni–Ti alloys [60].

Together with the kinetics study of cellular precipitation in Cu–Ti alloys the dissolving process of the sells was investigated too [61].
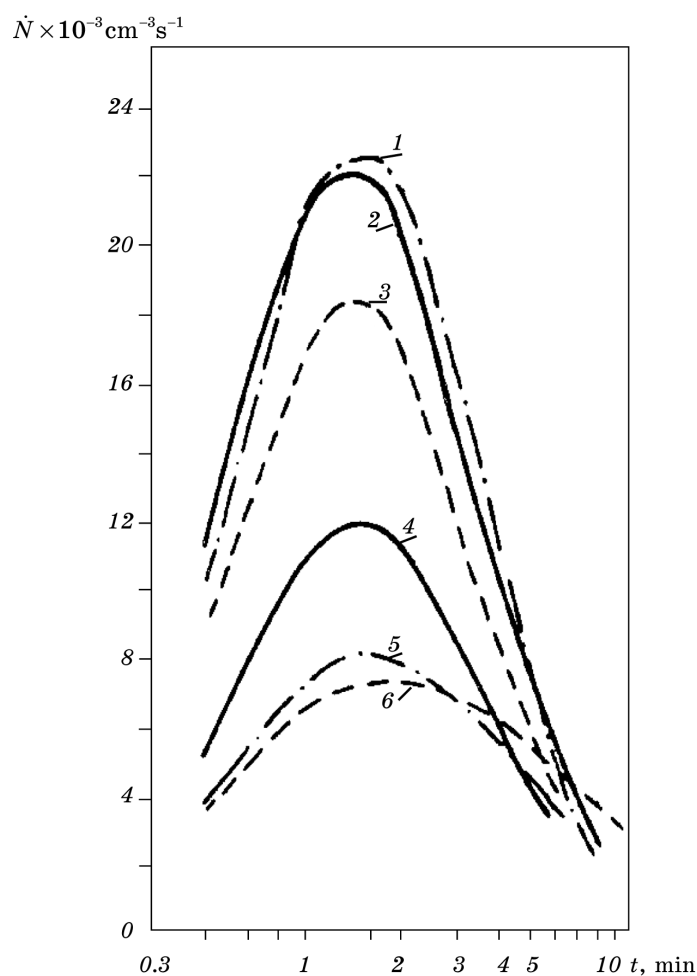
Fig. 15. The temporal dependence of the cells formation rate for temperatures: *1* — 650; *2* — 625; *3* — 600; *4* — 675; *5* — 700; *6* — 675°C. An alloy Cu−4.35 wt.% Ti [54].

For that Cu−5.7 at.% Ti alloy aged at 675°C was annealed at 820, 840, 850 and 870°C. At that, it was shown by X-ray analysis that in the temperature interval 817−867°C a dissolving of the cellular precipitates occurred by the discontinuous mechanisms. The metallography showed that such process has been carried out by reverse cells moving after recessive plates ends of the dissolving phase. Moreover, it was shown that both cellular precipitation and reverse dissolving were described by the same Arrenius' law — by the straight line. In this case the diffusion on the reaction front was the main controlling factor.

5. Alloying Elements Effect on Cu−Ti Alloys Aging

It well known that an addition of the third element to the aging binary alloy may change the decomposition kinetics and the structure of the precipitate [40]. On the one hand, it is explained by an interaction between atoms of the admixture and non-equilibrium vacancies and, on the other hand, this causes with the formation of new, as a rule, threefold precipitate. However, it is possible that the admixture does not change the precipitate structure and only alters its lattice parameters modifying the value of the misfit with a matrix lattice. Namely, that was observed in the Cu−5.92 at.% Ti alloyed with Ag (1.22), Be (1.37), Cr (0.6), Fe (0.54) and Zr (0.22 at.%) [62]. In such case an altering of the lattice constants of the Cu_4Ti phase was found (Table 1).

It should be born in mind that these constants were calculated in electrolytic extracted particles of the Cu_4Ti phase. As seen from Table 1 an addition of the Ag to the Cu−Ti alloy does not change the lattice constants of this phase whereas additions of Be, Cr and Fe reduce their values. For itself turn, Zr addition increases a constant and decreases c one of the Cu_4Ti phase. An alteration of these constants due to alloying of Cu−Ti alloys with foregoing elements leaded to change of the misfit values (Table 2) [62]. In this case the smallest misfit there is for Cr addition and for the direction of c axis

TABLE 1. The lattice constants of the Cu_4Ti phase in Cu−Ti base alloys [62].

Alloy	Lattice constants of the Cu_4Ti phase	
	a, nm	c, nm
Cu−Ti	0.3713	0.3634
Cu−Ti−Be	0.3696	0.3623
Cu−Ti−Ag	0.3713	0.3634
Cu−Ti−Zr	0.3718	0.3625
Cu−Ti−Cr	0.3690	0.3618
Cu−Ti−Fe	0.3696	0.3623

TABLE 2. Misfit values for the directions of a and c axis of the Cu_4Ti phase lattice [62].

Alloy	δ_a	δ_c
Cu−Ti	0.093	0.014
Cu−Ti−Be	0.076	0.003
Cu−Ti−Ag	0.093	0.014
Cu−Ti−Zr	0.098	0.005
Cu−Ti−Cr	0.070	−0.002
Cu−Ti−Fe	0.076	0.003

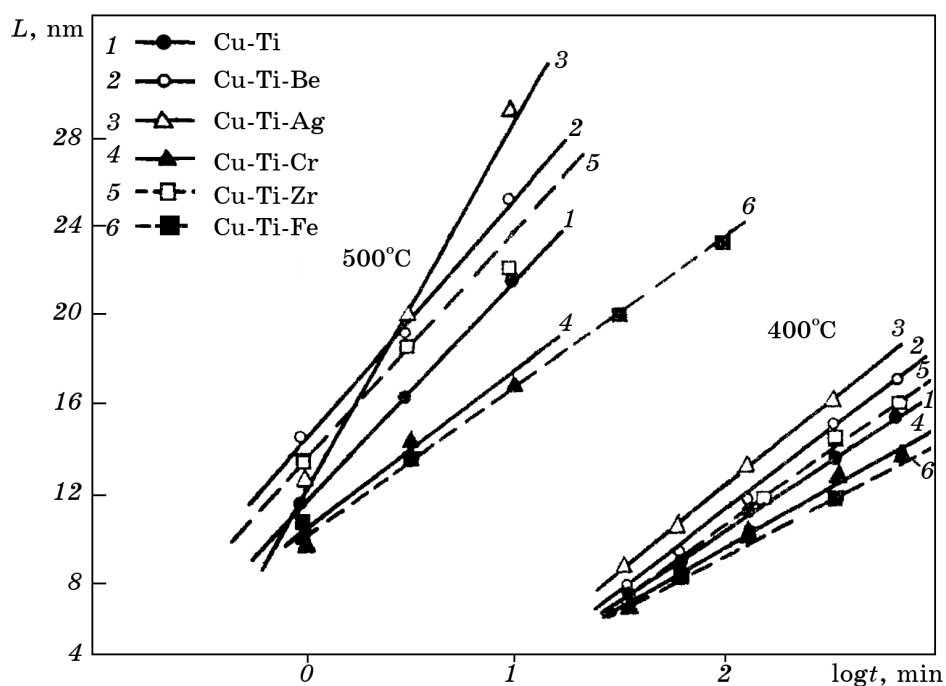**Fig. 16.** The kinetics of the middle sizes of the Cu_4Ti phase particles change in Cu–Ti base alloys at 400 and 500°C [62].
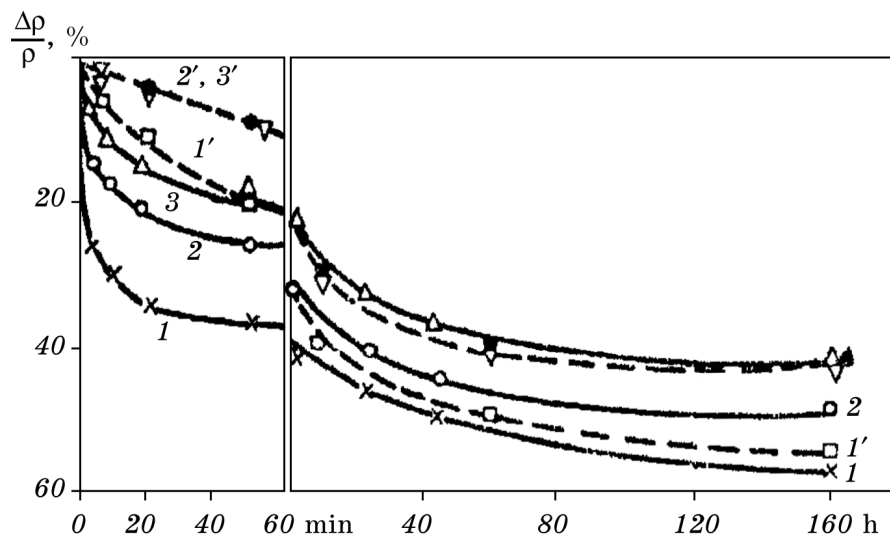

Fig. 17. The kinetics of the resistivity change at 340°C in Cu–Ti–Al alloys: numbers *1*, *2* and *3* are for alloys *1*, *2* and *4* correspondently; numbers *1′*, *2′* and *3′* are for alloys *1*, *2* and *4* quenched and deformed on 20% [63].

it changes even a sign. On the other hand, the Zr rises the δ_a value and reduces δ_c one. Summing up the information above, it appears that an alloying of Cu–Ti solid solutions with such quantity of hand-picked elements does not change the structure of the Cu_4Ti phase but introducing modifies into lattice constants. If it is the case, this effect has to influence on the kinetics of an enlargement of the Cu_4Ti phase particles. Indeed, as anticipated the rate of the growth of their middle size estimated from X-ray data (from the distances between satellites) depends on the kind of the alloying element (Fig. 16). As judged by this figure the highest rate of the particles growth may be observed in Cu–Ti–Ag alloy and the lowest one in Cu–Ti–Fe alloy at both temperatures where the misfit is smallest for a and c axis (Table 2). This agrees with the conclusion that the coarsening rate of the particles in aging alloys depends on the numerical value of the misfit [40].

For aging duration increase to 10 h at 500°C both the equilibrium β-phase and metastable α′-phase reflexes were found on the X-ray films. At that, the appearance of the β-phase reflexes depended on the alloy composition. First of all they were observed in Cu–Ti–Ag alloy (after 5 h at 500°C) while in other studied alloys these reflexes appeared after more longer time of aging at 500°C. Hence, the presence of the Ag in the Cu–Ti alloy provoked to the stable β-phase formation.

Interesting results were received in Cu–Ti alloys alloyed with the Al [63]. It was shown that the Ti solubility in Cu went down with the Al addition [64]. At the same time, in the threefold alloy Cu–Ti–Al the stable β-phase has the b.c.c lattice and the triple composition [65]. The authors of the work [63] investigated Cu–2.3 wt.% Ti–Al alloys with 1, 2, 3 and 5 wt.% Al labeled as *1*, *2*, *3*, *4* alloys correspondently. The kinetics curves of the resistivity change at 340°C are shown in Fig. 17. From these curves it follows that the phase transformation occurs without incubation period and its kinetics is extremely rapid with the rate continuously decreasing with a time. These peculiarities are typical for the homogenous precipitation with small activation energy of nucleation [40]. At that, this situation remains for alloys *1* and *2* at 500°C (Fig. 18) and is quite different for *3* and *4* ones where a transformation rate is smaller. It should be also noted that the mode of the kinetics curves of the alloys *1*, *2* and *3*, *4* are different that can be entirely explained in terms of the diverse activation energy of the nucleation [63]. We can only speculate at this time why in more concentrated Cu–Ti alloys with Al this phenomenon takes place because the structure of the precipitate and the mechanism of its formation at 500°C does not clarify. It is likely that this phase nucleates heterogeneously at this temperature.
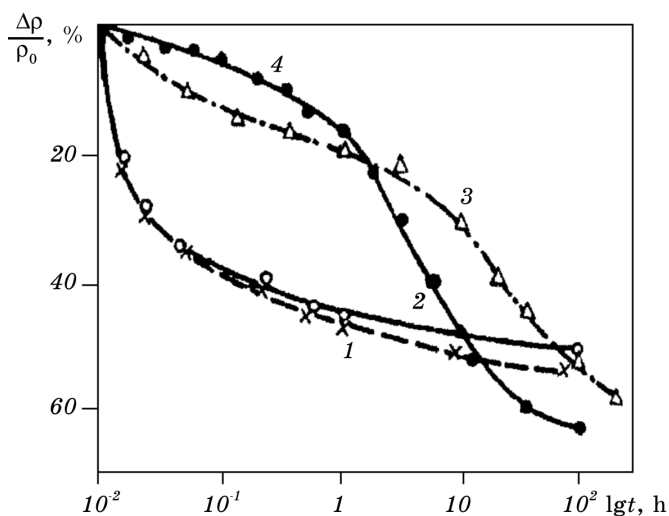
Fig. 18. Resistivity kinetics of Cu–Ti–Al alloys at 500°C after treatments: *1* — an alloy 2 quenched and deformed on 20%; *2* — an alloy 2 quenched; *3* — an alloy 3 quenched and aged at 450°C; *4* — an alloy 4 quenched [63].

An investigation of the Al addition effect on the discontinuous precipitation in Cu–Ti–Al alloys showed the following [63]. In alloys *3* and *4* this process did not realize in general. At that point, the precipitation of the triple phase at 500°C was carried out continuously on the defects. The discontinuous precipitation was observed in the alloy *1* and very seldom in the alloy *2*. In this case the volume fraction of such precipitation was less than in binary Cu–Ti alloy.

An alloying of the dilute Cu–Ti alloys with the big content of the Be (Cu–1.5 Ti–6.4 Be (I); Cu–2.7 Ti–3.4 Be (at.%) (II)) showed very interesting feature in the decomposition of these alloys [66]. The hardness measurement of quenched super saturated solid solutions during aging at different temperatures revealed two raises of this value (Fig. 19).

For understanding this phenomenon two binary alloys: Cu–12 at.% Be and Cu–5 at.% Ti were studied too. The temperature positions of hardness pikes of these alloys enabled to suppose that the first raise in threefold alloys corresponded to the Be precipitation and the second one — to the Ti precipitation. At the same time, however, both the modulate structure and metastable Cu_4Ti phase formation did not observe. Using of X-ray method for aged Cu–Ti–Be alloys showed the presence of the stable CuBe and Cu_3Ti phases reflexes only. If it was so then the cause of such high age-hardening response of the threefold alloys comparing with binary aged Cu–Ti alloys remained open.
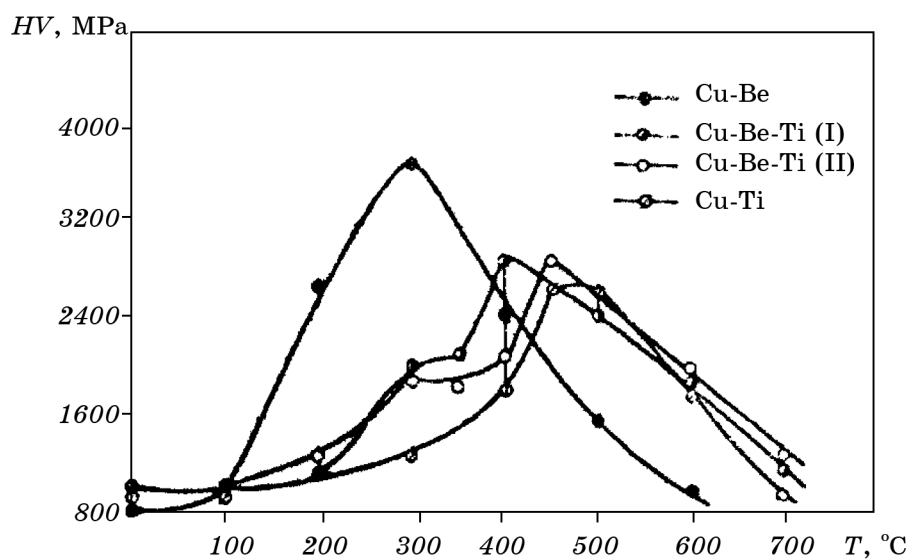
Fig. 19. Temperature dependence on the hardness change of the Cu–Be, Cu–Ti–Be (I), Cu–Be–Ti (II) and Cu–Ti alloys. The duration at the each temperature was 1 h [66].

It would be tempting to interpret this phenomenon as being the result of the high lattice distortion of a matrix due to CuBe phase precipitation that usually observed [40]. At that, the temperature interval of this phase formation coincided with the temperatures of the modulated structure formation in Cu–Ti alloy (350–400°C). An absence of the Cu_4Ti phase precipitation in aged Cu–Ti–Be was confirmed its luck in electrolytic extraction depositions where only the particles of the stable phases CuBe and Cu_3Ti were discovered. Moreover, an effect of the strain distortions in a matrix due to CuBe phase precipitation on the probability of the metastable Cu_4Ti phase formation may be ratified still more that plastic deformation of the Cu–Ti alloys with modulated structure or Cu_4Ti precipitates. As it will be showed at the next part of this paper the plastic deformation can also destroy these structure states in favour of the stable phase formation.

6. Effect of the External Influences on the Precipitation in Cu–Ti Alloys

6.1. Plastic deformation

An effect of plastic deformation on age-hardened Cu–Ti alloys was studied both in quenched and in aged alloys [48, 63, 68, 69]. It was

shown [48] that prior deformation of the quenched Cu−4.7 wt.% Ti alloy ($\varepsilon = 50\%$) has resulted in only small decrease of the resistivity during the decomposition at 400°C (Fig. 12, curves *2, 3*) but large decrease has been observed after 50% deformation and aging at 500°C (Fig. 12, curves *7, 8*). It is interesting that in threefold Cu−Ti−Al alloys (Fig. 17, curves *1′, 2′* and *3′*) the considerable deceleration of the resistivity lowering took place comparing with non-deformed quenched and aged alloys at 340°C. However, in the case of Cu−Ti−Al alloys deformed and aged at 500°C (Fig. 18) the rate of the resistivity change was much more than in non-deformed ones. These results earnestly showed that crystalline defects created due to plastic deformation had less effect on the solute-rich complexes formation and more effect on the discontinuous precipitation that occurred at 500°C [48].

One of the first studying of the plastic deformation effect on the aged structure of the Cu−Ti alloy by X-ray method showed the following [68]. After plastic deformation (a tension on 10% and above of the wire-sample in X-ray chamber) of the Cu−4.5 wt.% alloy aged for 150 min at 450°C the modulated structure destroyed (the satellite reflexes vanished) and two-phase structure $\alpha + \beta$ was observed only. On the other hand, if the Cu−Ti alloy aged for 60 min at 500°C and contained Cu_4Ti phase to put on the plastic deformation (a rolling on 33% and above) two-phase structure $\alpha + \beta$ was identified by X-ray too. For more detailed analysis of the plastic deformation effect on the structure of the Cu−Ti alloy aged and deformed samples were electrolytic dissolved and the obtained particles were identified by X-ray analysis [68] (Table 3).

As seen in Table 3 in the contrary to the X-ray analysis of the bulk samples where reflexes of $\alpha′$-phase (Cu_4Ti) did not find, in the extracted particle they were detected due to the volume fraction of this precipitate was very small in the first case.

From these results the main feature has to be noted. The compositions of the solute-rich regions of the modulated structure, intermediate metastable $\alpha′$-phase and the stable β-phase probably are close one another and the transition one structure to other is the diffusionless transformation.

An effect of the plastic deformation on the aging kinetics in Cu−Ti alloy was analyzed in [69]. It was found that the modulation period and the rate of its growth during aging at 430 and 500°C were smaller than in non-deformed alloy. However, the rate of precipitation and coarsening of the $\alpha′$-phase in the deformed alloy was bigger (Table 4). Indeed, as seen from the Table 4 an increasing of the deformation degree leads to the acceleration of the $\alpha′$-phase particles growth.

To study of the plastic deformation effect on aged state Cu−4.5 Ti

TABLE 3. The composition of the electrolytic extracted particle (e.p.) from the aged and aged and deformed Cu–Ti alloy [68].

No.	Treatment	The composition of e.p.
1	400°C, 1 h	−
2	400°C, 1 h + ε = 50%	α′ + β
3	400°C, 1 h + ε = 50% + 400°C, 1 h	α′ + β
4	500°C, 1 h	α′
5	500°C, 1 h + ε = 34%	α′ + β
6	500°C, 1 h + ε = 34% + 400°C, 1 h	α′ + β

TABLE. 4. The dependence of the α′-phase particle size (L) on the aging time at 500°C and on the degree of the plastic deformation of the Cu–4.5 wt.% Ti alloy [69].

No.	Aging time, min	$T_a = 500°C$ L, nm	ε = 22% + 500°C L, nm	ε = 44% + 500°C L, nm
1	Quench. + deform.	−	−	−
2	1	6.0	4.6	5.0
3	5	7.2	−	6.4
4	10	−	6.0	6.0
5	40	21.4	50.0	6.4
6	100	64.0	83.5	95.0
7	300	80.0	125.0	140.0
8	600	95.0	−	−

TABLE 5. X-ray phase analysis data of the Cu–5 Ti–0.5 Cr (wt.%) after aging and deformation [69].

No.	Alloys treatment	Alloy phase state	Q, nm
1	400°C, 120 min	α-phase + m.s.	19.0
2	400° + def. 1.8%	α-phase + m.s.	19.5
3	400° + def. 6.8%	α-phase + m.s.	19.0
4	400° + def. 13.2%	α-phase + m.s.	18.5
5	400° + def. 24.7%	α-phase + m.s.	15.0
6	400° + def. 38.0%	α + α′	−
7	400° + def. 58.0%	α + α′	−
8	400° + def. 75.5%	α + α′	−
9	500°C, 60 min	α + α′	−
10	500° + def. 20%	α + α′	−
11	500° + def. 28%	α + α′	−
12	500° + def. 42%	α + α′ + β	−
13	500° + def. 64%	α + α′ + β	−

and Cu−5 Ti−0.5 Cr (wt.%) alloys were picked out. The preliminary aged at 400 and 500°C alloys were deformed by rolling The phase transformations occurred in Cu−Ti alloys may be represented as follows: aging at 400°C, 60 min + deformation $\varepsilon = 10\%$ and above: $\alpha + $ m.s. $\rightarrow \alpha' + \beta$; aging at 500°C, 60 min + deformation $\varepsilon = 35\%$ and above: $\alpha + \alpha' \rightarrow \alpha' + \beta$.

The phase transformations in the threefold alloy after aging and plastic deformation are characterized by some different features. The results of the X-ray investigation of this alloy after aging and deformation are reported in the Table 5. In this table m.s. — modulated structure; α — phase-matrix; Q — period of the modulation. The data in this table testifies to a fact that small degrees of the deformation have a little influence on the period modulation growth. And only after $\varepsilon = 38\%$ of the deformation the satellites have flanked the main reflexes disappeared and the α'-phase lines are observed on the X-ray photograph.

For more detailed understanding of the deformation effect on aged structure of Cu−Ti and Cu−Ti−Cr alloys coarse-grained samples were studied by X-ray method [69]. In this case aged samples were deformed in a X-ray chamber directly so as it was possible to get the reflexes from the same grain. It was shown that already small deformation by tensile on 4.2% leaded to decreasing of the satellites intensity and 6.3% provoked the disappearance of the satellites in Cu−Ti alloy. At the same time, the diffuse reflexes of the metastable α'-phase was observed. Comparing these results with the case of rolling deformation when the satellites disappeared for 38% allowed to say that the tensile deforming influences on the structure change more effective. On the other hand, disappearance of the satellites in the Cu−Ti−Cr alloy occurred after bigger deformation degree (38%) than in the Cu−Ti (10%).

A disappearance of the satellites as a result of the plastic deformation was explained by a loss of the coherency of the Ti enriched regions of the modulated structure due to moving dislocations which transform the coherent interface to non-coherent or semicoherent at the plastic deformation [40]. In this case two possibilities may be realized: or the X-ray optical coherence was broken and the independent reflexes of α'-phase appeared in such situation, or enriched regions of the modulated structure transformed in the partly-coherent particles of the Cu_4Ti phase due to an interaction with the dislocations. The first possibility causes thereby the presence of the X-ray diffuse scattering exists if the optical coherence usually keep safe [41]. On the other hand, in aged Cu−Ti alloy containing metastable α'-phase the plastic deformation causes the transition this precipitate into stable phase. This may points out to the closeness of the composition of the both phases.
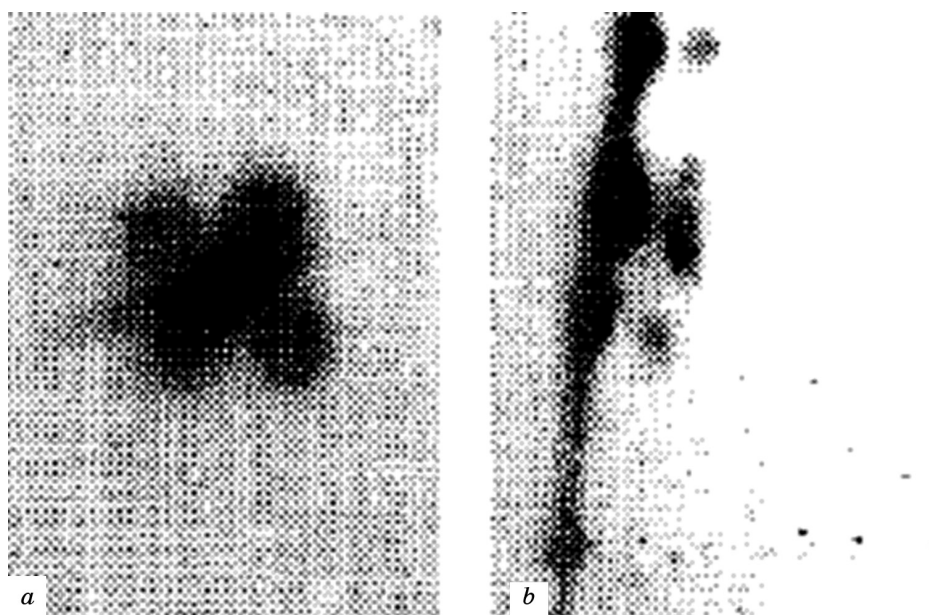
Fig. 20. The fragments of the X-ray picture in an alloy Cu–3.5 wt.% Ti, aged at 500°C for 3 min: a — satellites flanked the matrix reflex 111; b — after USD ($I=100\,\text{W/cm}^3$, $t=3\,\text{min}$), Cuk_α radiation. Magnification ×8 [71].

An investigation of the plastic deformation influence by rolling ($\varepsilon=10-75\%$) on the cellular precipitation in Cu–5.7 at.% Ti alloy showed that after $\varepsilon = 20\%$ and aging for 25 min at 575°C the abrupt acceleration of this transformation took place [70]. In such case the cell nucleation happened both on the grain boundaries and inside of the grains. The X-ray analysis showed that recrystallization nucleuses have formed before cell nucleation ocurred inside the grain and possibly have provoked the cell reaction. Consequently, a number of the nucleation places for cells increased essentially that together with improving of the reaction front mobility due to the multiplication of the grain-boundary dislocations leaded to such big deformation effect on the cellular precipitation.

Summing up the information above, it appears that plastic deformation of the aging Cu–Ti alloys exerts small influence on the rate of the modulated structure evolution but can produce considerable structural change in the aged and deformed alloy: destroying of the modulated structure and contribute to the transition of the metastable α'-phase into stable β-phase. Furthermore, the plastic deformation enlarges essentially the rate of the cellular precipitation due to the acceleration both the cell nucleation and the reaction front mobility.

6.2. Ultra-Sonic Deformation

It well known that the ultra-sonic deformation (USD) has a big influence upon the structure, properties and the precipitation kinetics of age-hardened alloys [71]. As rule, introducing a high defects density into an alloy accelerates the heterogeneous nucleation of the precipitate thus increases the decomposition rate. For elucidation the possible effect of USD on the precipitation processes in quenched Cu−Ti alloy with 3.5 wt.% Ti was selected [72]. Ultra-sonic irradiation treatment (USIRT) was conducted in the Cu−Ti alloy both after quenching and after aging at 400°C, 30 min or at 500°C, 3 min. In the last case an alloy contained the modulated structure. In these cases USIRT was carried out at the temperatures closed to an ambient one. The peak power was 40−100 W/cm^2 and the duration of a radiation changed from 2 to 30 min. It was shown that the USIRT during 2−12 min of the quenched alloy did not change visibly the terminal alloy structure: the mode of the X-ray diffuse scattering (satellites intensity and their position) remained unchanged (Fig. 20, *a*). Simultaneously the small (3−4 nm) coherent regions enriched with Ti were observed by TEM [29].

However, the dislocation structure transformed, at that the dislocation density increased and the dislocation distribution became more not uniform. This caused the small hardness growth but the hardness increment did not exceed 20% (Fig. 21, curve *1*). Moreover, USIRT of the aged at 400°C, 30 min Cu−Ti alloy containing the coherent complexes enriched with Ti altered the hardness even smaller (Fig. 21, curve *2*). In a work [72] such situation was explained by an insufficient value of the peak power of USD for strengthening already age-hardened alloy. In such case the high
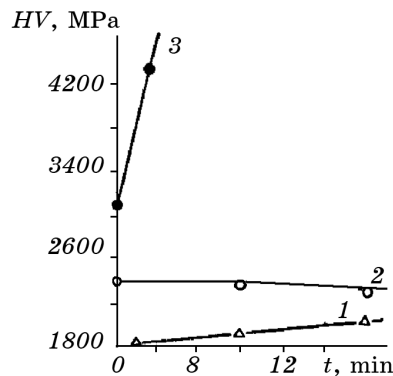

Fig. 21. The hardness dependence on the ultra-sonic irradiation time in Cu−3.5 wt.% Ti alloy: *1* — quenched state; *2* — after aging at 400°C, 30 min; *3* — after aging at 500°C, 3 min [71].

internal coherent strains would made the obstacles in the way of dislocations moving but only their multiplication was looked. Perhaps, in this case a sum of the stresses due to USD and internal coherent distortions did not exceed the yield stress of the aged alloy and therefore USD strengthening was absent. Quite the contrary, when this sum preceded the yield stress of the alloy aged at 500°C, 3 min the hardness increment was very high (Fig. 21, curve *3*). At that time matrix reflexes 111 on the X-ray film revealed the tangential broadening (Fig. 21, *b*) that pointed to the growth of the disorientation of the adjacent crystalline micro-regions of the matrix. Usually this stimulates the dislocation density increase and additionally deformation strengthening consequently (Fig. 21, curve *3*). It should also be noted, that after USIRT an alloy preliminary aged at 500°C, 3 min the satellites disappeared and the reflexes of metastable α'-phase were observed. It permits to suppose that similarly to the plastic deformation USIRT or destroyed the modulated structure breaking the structural coherence of the Ti enriched regions, or disturbed of the optical coherency causing the diffuse scattering disappearance.

Since in a case mentioned above the USIRT was conducted at ambient temperature it would be interested to realize that treatment at aging temperature [73]. For that an alloy Cu−3.5 wt.% Ti was treated by USD with the intensity 150 MPa/mm^2 less than the yield stress of the quenched alloy ($\sigma_{0.2} = 200$ MPa/mm^2). So, in the alloy after USD treatment at the temperature of the modulated structure formation ($T = 370$°C) the diffuse scattering — satellites remained but the rate of the period modulation growth was greater than for non-irradiated alloy at 400°C (Fig. 22, *a*). At the same time, the hardness of the aged alloy under USD increased faster. The USD at the aging temperature 470°C when the metastable α'-phase usually precipitated stimulated very high age-hardening effect — the hardness achieved the value far more than in an alloy aged at 500°C without USD (Fig. 22, *b*).

These results were explained by two operating factors in such case: the contribution in the strengthening due to a presence of the coherent α'-phase particles after aging and the grain-boundary hardening as the result of dislocation walls formation near these precipitates [73, 74]. It is interesting to note that such gigantic hardening effect under USD at 470°C. was observed in a very narrow time interval. Indeed, with the increasing of aging time at that temperature the rapid overaging occurred (Fig. 22, *b*, curve *1*). At the same time, an increasing of an aging duration at 500°C without USD leaded to further strengthening (Fig. 22, curve *2*). Such phenomenon may be explained as follows. It should be born in mind that USD initiates an origin the large dislocation density and promotes their
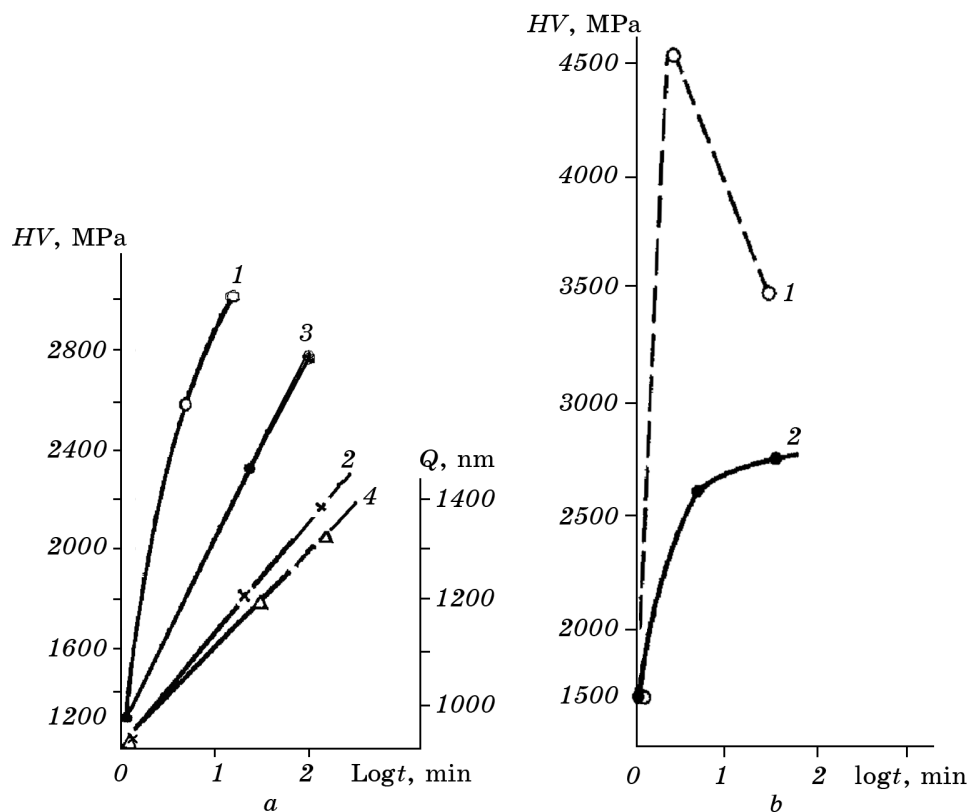
Fig. 22. Effect of the USD on age-hardening response of the Cu–3.5 wt.% Ti: *a* — time dependence of the hardness of an alloy aged at 370°C under USD (*1*); the same of the modulation period (*2*); (*3, 4*) — the hardness and the modulation period dependence at 400°C without of USD consequently; *b* — hardness kinetics at 470°C under USD (*1*); the same at 500°C without of USD (*2*) [73].

moving, as rule [75]. Moreover, this treatment resulted to the vacancy concentration rising too [76]. Consequently, the aging under USD had to proceed with more rate and the coherency loss become sooner due to dislocation attraction to the interface. It should be underlined that the similar effect of USD was described in age-hardened Cu–Be alloy [77].

6.3. Effect of the Uniform Pressure on the Cellular Decomposition in Cu–Ti Alloys

It is known that high pressure may essentially change the rate of the diffusion in solids [78]. It was interesting to study the effect of the
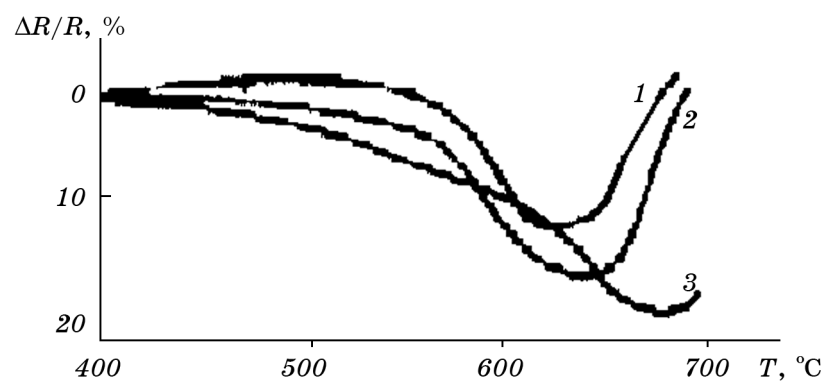
Fig. 23. The temperature dependence of the resistivity of the Cu–5.3 at.% Ti alloy under a pressure: *1* — 1.5; *2* — 2.54; *3* — 3.7 GPa [79].
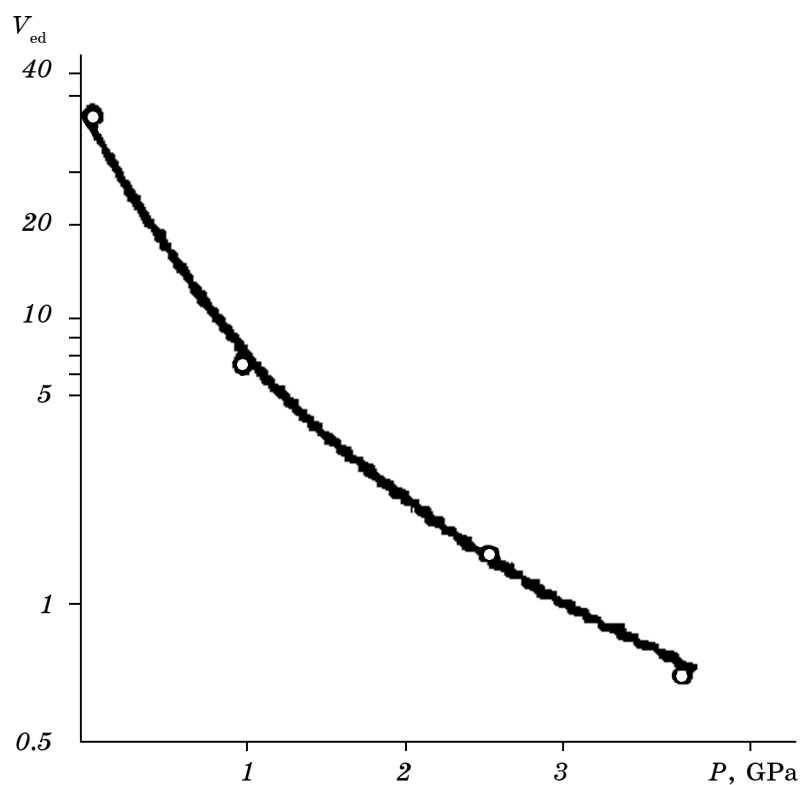

Fig. 24. The dependence of the volume occupied by cellular decomposition (V_{cd}) on a pressure in the alloy Cu–5.3 at.% Ti aged for 24 min at 625°C [79].

uniform pressure on the kinetics of the cellular precipitation in Cu−5.3 at.% Ti alloy [79]. In this case the quenched alloy was aged under pressure 1−7.5 GPa at 550−770°C. As a consequence of this a resistivity diminution started at more less temperature at increasing the pressure meaning (Fig. 23). But the metallography analysis showed that this result did not correspond to the acceleration of the cellular decomposition since the volume occupied by cellular decomposition (V_{cd}) reduced with a pressure increased (Fig. 24). Moreover, at the pressure 4 GPa the cellular precipitation was retarded fully. The observed acceleration of the resistivity under a pressure was explained by the reduction of the Ti solubility that was typical for many solid solutions being put under the pressure [78].

In this connection a pressure increasing was accompanied by lowering of the solubility of the Ti in the Cu and as a result the general decomposition started at lower temperature that diminishes the volume of the cellular precipitation [57]. Contrary to the atmosphere pressure an overpressure reduced the rate of the front cell displacement but with a temperature rise this effect become smaller [78]. For example, if a pressure 3.7 GPa at 625°C reduces this value in 25 times so at 670°C it diminishes under the same pressure only in 9.3 times. This effect of pressure on the rate of cellular decomposition has been explained, as the calculation showed, by essentially decreasing of the diffusive mobility of Ti atoms on the grain boundaries [78]. At the same time, for the development of the cellular decomposition a reconstruction of the grain boundary plays a big role in this process [80]. The overpressure retards such transformation and in that way reduces the cellular decomposition velocity.

6.4. Effect of Radioactive Irradiation on Precipitation in Cu−Ti Alloys

The results of the radioactive irradiation effect on the precipitation phenomenon were discussed by many authors [40]. In the case of Cu−Ti alloys this phenomenon was investigated in Cu−Ti solid solutions containing 4.0 (1) and 6.0 wt.% Ti (2) [81]. The quenched samples of these alloys were irradiated as following: the alloy (1) — by neutrons with the fluence $2.34 \cdot 10^{22}$ n·m^{-2} and the alloy (2) — by electrons with an energy 2.5 MeV and the fluence $1 \cdot 10^{22}$ and $5 \cdot 10^{22}$ e·m^{-2}. An effect of the radioactive irradiation on the cellular decomposition was studied mainly. At that, a value of the volume occupied by cellular decomposition (V_{cd}) depending on the irradiation nature and an aging duration was determined. An alloy (1) irradiated by neutrons was aged at 600°C. As seen in Fig. 25, a value V_{cd} is less in irradiated alloy (1) than in radiation-free one at the same aging regime. So, for aging time 420−1980 min such difference is 20%. The same effect was observed in an alloy (2) irradiated by electrons and aged
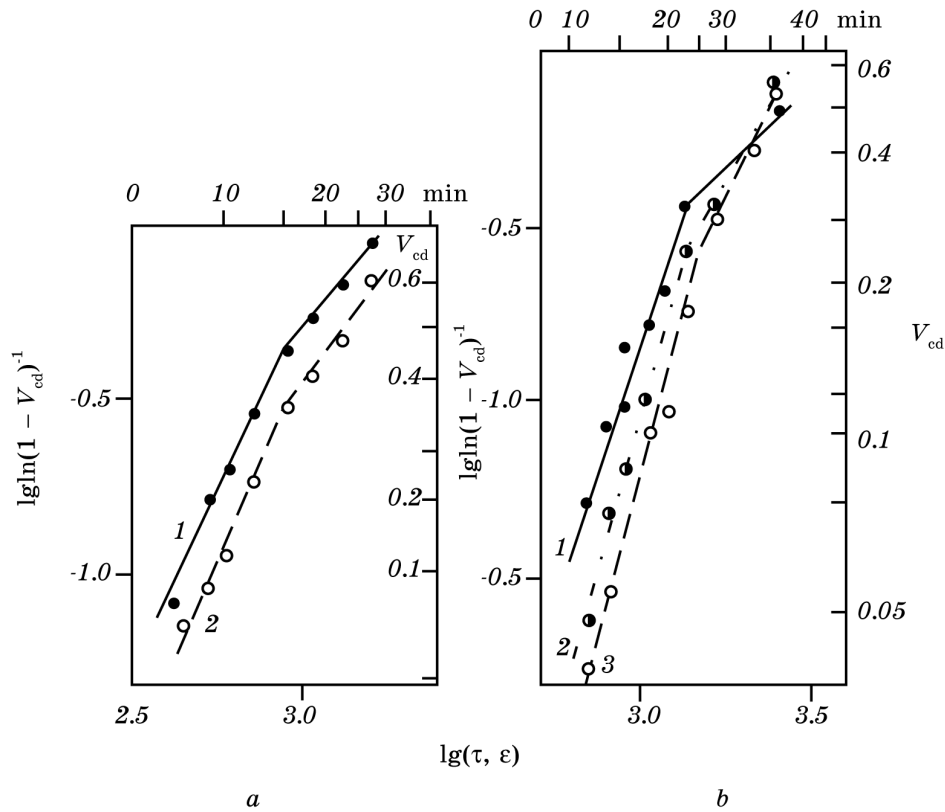
Fig. 25. The dependence of the cell decomposed volume Vcd on the aging duration in Cu−Ti alloy: *a* — an alloy (*1*) at 600°C: *1* — irradiated-free; *2* — neutron irradiated; *b* — an alloy (*2*) at 575°C: *1* — irradiated-free; *2* — electrons irradiated ($F = 1 \cdot 10^{22}$ e.m.$^{-2}$); *3* — $F = 5 \cdot 10^{22}$ e.m.$^{-2}$ [81].

at 575°C (Fig. 25, *b*). In such case the decreasing of V_{cd} depended on the electron fluence (*F*) and was equal 37% at $F = 1 \cdot 10^{18}$ sm^{-2} and 47% at $F = 5 \cdot 10^{18}$ sm^{-2}. The curves in Fig. 25 have two plots each of those may be described by an equation [50]

$$V_{cd} = 1 - \exp(-Kt^n), \qquad (4)$$

where *K* is a constant of the transformation rate and *n* is an exponent depending on the mechanisms of the nucleation and a growth of the new phase centers. The lower plots in Fig. 25 are determined by the nucleation and the growth of these centers and the upper ones (after a curves bend) are characterized by their growth only. The values of *K* and *n* calculated for the both plots in Fig. 25 are represented in Table 6.

TABLE 6. Dependence of the values K and n in equation (4) on the neutrons irradiation dose in Cu−Ti alloys [54].

Alloy	$F \cdot 10^{22}$	n_1^*	n_2^*	K_1	K_2	$v \cdot 10^7$ m/s
Cu−4 Ti	0	2.06	1.23	2810	80.2	4.7
	2.34 n/m^2	2.12	1.34	1290	25.4	3.2
Cu−6 Ti	0	2.89	1.00	2.72	229.0	4.9
	1.00 e/m^2	3.63	1.78	0.009	0.61	0.68
	5.00 e/m^2	3.70	1.99	0.004	0.11	0.38

As seen from Table 6 the irradiation decreases appreciably the cellular decomposition, at that this effect increases with rising of irradiation dose. In an alloy Cu−4 Ti the neutrons irradiation did not change the relation between the nucleation and growth rates of new phase since the n value small changed in this case [82]. Using the K_2 values and the following equation [60]

$$v = (3K/4\pi\bar{N})^{1/3}, \tag{5}$$

the rate of the cells growth has been calculated (Table 6) [54]. These results lead to the thought that both neutrons and electrons irradiation retard the migration of the front of the cellular decomposition. Moreover, an irradiation creates the radiation defects in quantity that initiates the precipitation internal grains that in part reduces the cellular decomposition. However, an analysis of the data obtained by X-ray microprobe technique showed that the main effect of the irradiation on cellular reaction caused by the resolution of the grain-boundary segregations during an irradiation [54].

7. Mechanical Properties of Aged Cu−Ti Alloys

It was found that Cu−Ti aging alloys are characterized by large age-hardened response. It was discovered on the onset of their investigation [3, 4]. Having high-strength and high-conductivity properties these alloys can replace successfully the well-known beryllium bronze in numerous applications [2]. The main reason of high-strength properties of Cu−Ti alloys is the modulated structure formation composing the coherent fine-scale particles of the metastable Cu_4Ti phase [2, 13, 33, 49]. The kinetics of the age-hardening and the slip mechanisms were investigated in Cu−4.7 Ti (1); Cu−2.3 Ti−2 Al (2) and Cu−2.3 Ti−5 Al (wt.%) (3) alloy [49]. In this case a change of the yield stress ($\sigma_{0.1}$) and the strengthening coefficient ($\Theta_{0.2}$) were measured after isothermal aging at 340, 400, 450 and 500°C. Parallel with that the mode of the slip was looked too.
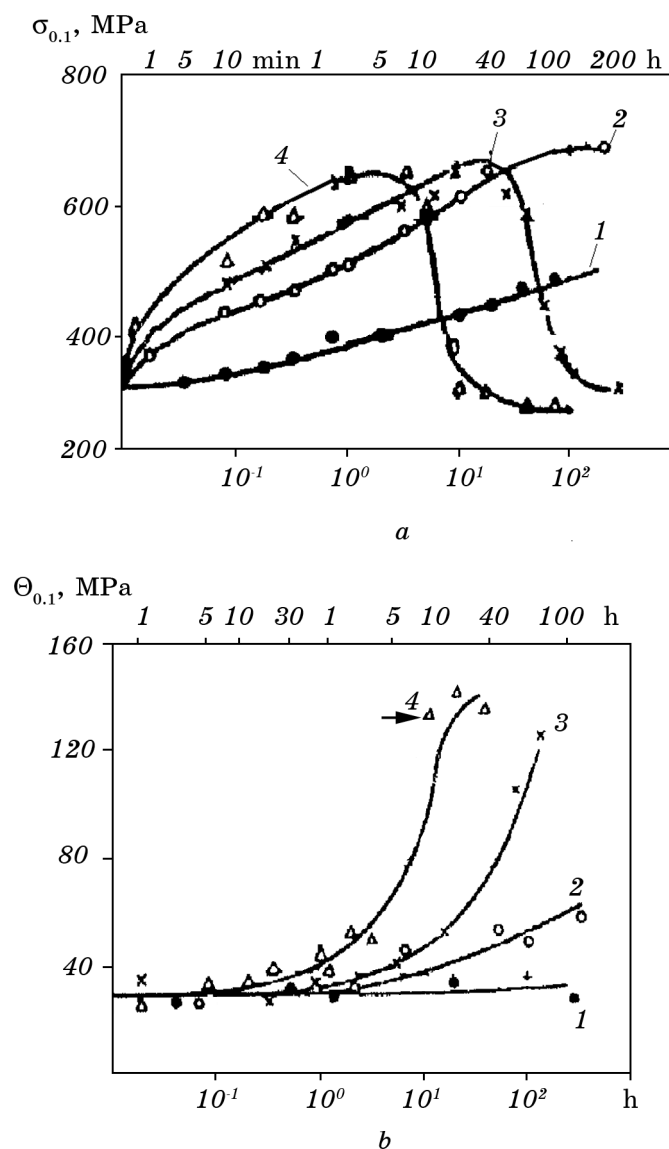
Fig. 26. The kinetics of $\sigma_{0.1}$ — *a* and $\Theta_{0.1}$ — *b* of an alloy 1 at following temperatures: *1* — 340; *2* — 400; *3* — 450; *4* — 500°C [49].

The obtained results are summated in Fig. 26 and 27. It may be deduced that an aging at 340°C of the alloy 1 leads to noticeable promotion of the yield stress without change of the strengthening coefficient ($\Theta_{0.2}$) (Fig. 26, *a, b,* curve *1*). The similar results were received in an alloy 2 (Fig. 27). At the same time the changing of
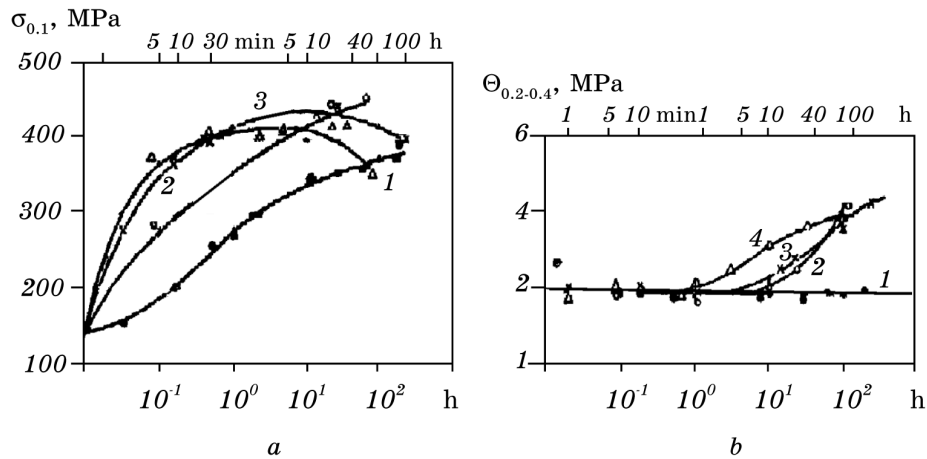
Fig. 27. The kinetics of $\sigma_{0.1}$ — a and $\Theta_{0.1}$ — b of an alloy 2 at following temperatures: *1* — 340; *2* — 400; *3* — 450; *4* — 500°C [49].

$\sigma_{0.1}$ at $\Theta_{0.2}$ = const, were noticed at the aging temperature increasing only from the onset of the decomposition (at $T \leq 450$°C up to 1 h). At this point, the value of $\sigma_{0.1}$ achievs the maximum in the alloy 3 (Fig. 26). It should be also noted that in alloys 1 and 3 a value $\Theta_{0.2}$ increased greatly only on the overaging stage but in alloy 2 for maximal value of $\sigma_{0.1}$. According to the modern points of view the condition $\Theta_{0.2}$ = const corresponds to the cutting of coherent precipitates by the dislocations that confirm by structural investigations [40]. For understanding the possible strengthening mechanisms in Cu–Ti alloys during aging in [49] has been proposed that the main hardening factor was internal coherent stresses. In such case an estimation of the increment of $\sigma_{0.1}$ due to aging ($\Delta\sigma$) on Mott–Nabarro's model was showed $\Delta\sigma \approx 300$ MPa and the experimental value was 450 MPa. That difference was explained by the contribution the grain-boundary factor into the strengthening effect taking into account additionally the precipitation of the stable β-phase on the grain boundaries [49]. An analysis of the phase and structural states of the Cu–Ti alloys corresponding to the sharply falling of $\sigma_{0.1}$ and promoting of $\Theta_{0.2}$ directed on the partly loss of the coherency of the metastable Cu_4Ti phase [49].

The character of the interaction between precipitates and dislocations in the deformed Cu–Ti alloys may be determined by the metallography [49] (Fig. 28). So, in a quenched state the uniform distribution of the slip was observed in the grains but with strong localization of the shear in the slip bands (Fig. 28, *a*). Aging at 450–500°C for $t < 30$ min did not change this picture although the yield stress has achieved its maximal value. As it was mentioned above, this sit-
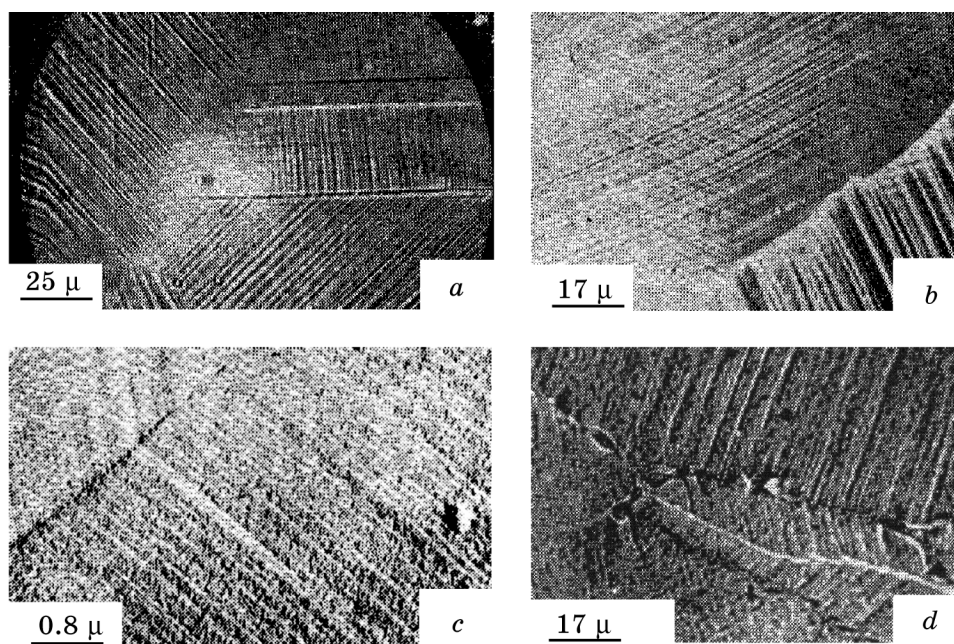
Fig. 28. The mode of the slip bands in an alloy 3 after treatments: *a* — quenching and deformation ε = 6%; *b* — aging at 500°C for 20 min; *c* — an alloy 1 quenched, deformed on ε = 2% and aged for 10 h at 450°C; *d* — an alloy 3 quenched, deformed on ε = 6% and aged for 95 h at 500°C [49].

uation corresponds to cutting of precipitates by dislocations that probably did not change the mode of the slip (Fig. 28, *b*). The is very interesting fact since until now a transition from quenched state to fine-scale two-phase system usually was accompanied by sharply slip localization [40]. Perhaps it may be explained as follows the more such investigations were conducted in Al-base alloys where the stacking fault energy was higher than in Cu-base ones. Increasing an aging duration leaded to an appearance of the broad slip bands that clearly were detected by TEM (Fig. 28, *c*). The outward character of these bands looks like the deformation twins that was confirmed experimentally [82]. Thus, the feature of the deformation mechanisms near the maximum age-hardening response is the mechanical twining appearance and transition to more fine slip.

It should be highlighted that in Cu—Ti—Al alloys the dislocation cross-slip near the precipitates did not find that was an evidence of dislocation bypassing these particles due to Orovan's mechanisms [49]. The metallography study of the overaged states in alloys 2 and 3 showed that at small deformation degree slip lines were very fine and therefore did not detect. But for larger deformation (ε = 6—9%)

TABLE 7. Mechanical and electrical properties of the aged Cu−4.8 wt.% Ti and Cu−2 wt.% Be [83].

Property	Cu−Ti	Cu−Be
Specific electrical resistance, o/mm^2/m	0.064	0.065
Compressive strength, MPa	1460	1500
Young's modulus, GPa	130	132
Relative elongation, %	4−15	3.0
Vickers's hardness, MPa	3600	4000
Cyclical strength of membranes at $P = 100$ at.	13200	11000

the slips with the rough, discontinuous slip trace were observed (Fig. 28, *d*). As anticipated, the internal coherent stresses were the main reason of the age-hardening response of Cu−Ti alloys as a result of metastable Cu$_4$Ti phase precipitates forming the modulation structure. An additional factor may be an energy expense for destroying of the ordered structure of the Cu$_4$Ti phase and on the creation of a new interface. It is necessary to underline the mechanical twinning observation in aged Cu−Ti alloys was not looked earlier [49].

A comparison of the Cu−Ti alloy mechanical and electrical properties with the same properties of the beryllium bronze showed that Cu−Be alloy may be replaced by Cu−Ti one in success (Table 7) [83].

8. Reversion Phenomenon in Cu−Ti Alloys

As everybody knows, the main reason of a reversion in age-hardening alloys is the temperature stability of the low-temperature decomposition products [40]. At the same time, this process determines the effectiveness of the two-step aging in many respects. For example, in alloys where a reversion becomes apparent in the large degree an effect from two-step aging will be negligible [84].

The reversion phenomenon in Cu−5 at.% Ti alloy was studied in [85]. The preliminary aging was at $T_a = 400°C$ for 30 and 600 min, at $T_a = 500°C$ for 30 min and 10 h, at $T_a = 550°C$ for 30 and 300 min. These treatments allowed to get the coherent (aging at 400°C) or semi-coherent (aging at 500 and 550°C) precipitates of the metastable Cu$_4$Ti phase. The reversion kinetics of the hardness was researched at $T_r = 600$ and 700°C (Fig. 29). Simultaneously with the hardness reversion the structural changes in the alloy after a rever-
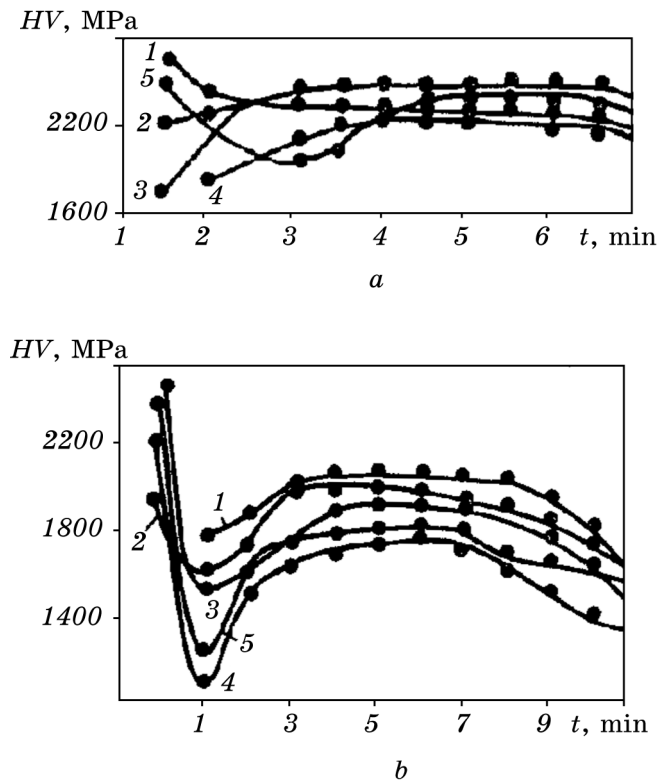
Fig. 29. The kinetics of the hardness reversion in Cu–5 at.% Ti alloy at $T = 600°C$. (*a*) aged at the temperatures: *1* — 500°C, 10 h; *2* — 550°C, 30 min; *3* — 400°C, 30 min; *4* — aging at 600°C; *5* — 400°C, 10 h; the same at 700°C (*b*) after aging at the temperatures: *1* — aging at 700°C; *2* — 400°C, 30 min; *3* — 550°C, 30 min; *4* — 500°C, 10 h; *5* — 400°C, 10 h [85].

sion were studied by the X-ray and TEM investigations (Fig. 30 and 31). It was shown that the partly reversion at $T_r = 600°C$ occurred only for an alloy aged at $T_a = 400°C$ for 30 min and at $T_a = 500°C$ for 30 min (Fig. 29, *a*). For other cases the hardness rose at reversion temperature. However, at $T_r = 700°C$ the reversion was observed at every T_a (Fig. 29, *b*). The X-ray investigation of the Cu–Ti alloy coarse-grained sample showed that if after aging at $T_a = 400°C$ for 30 min the satellites flanked the main reflex were present so after heating at 775°C the reflexes from metastable Cu_4Ti phase were visible only (Fig. 30, *a*, *b*). At that, the number of these reflexes corresponded to the number of tetragonal phase orientations to the cubic matrix. After annealing at 775°C for 1 min preliminary aged alloy at 550°C, 30 min some transformation of the Cu_4Ti phase reflexes observed (Fig. 30, *c*, *d*). TEM study of the Cu–Ti alloy aged
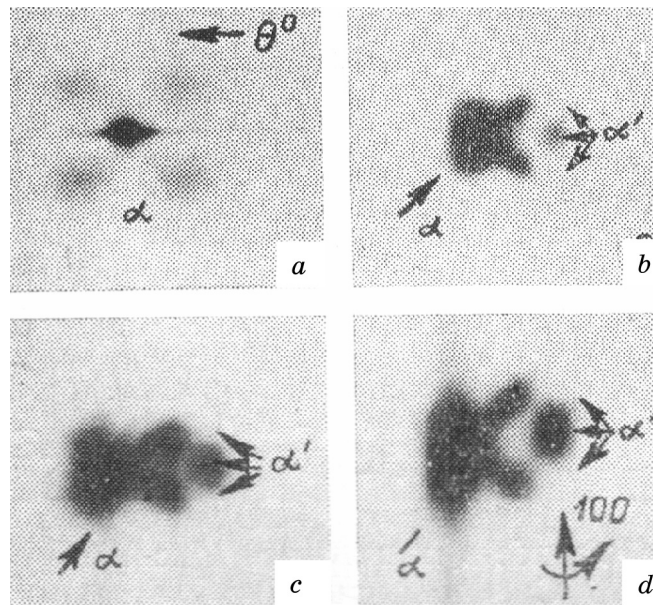
Fig. 30. The transformation of the diffuse scattering near the matrix reflex 220 on the oscillated film from the coarse-grain sample of the Cu−5 at.% Ti alloy trated the following manner: *a* — 400°C, 30 min; *b* — 400°C, 30 min + 775°C, 1 min: *c* — 550°C, 30 min; *d* — 550°C, 30 min + 775°C, 1 min. Cuk_α — radiation [85].

at $T_a = 400$°C for 30 min and $T_a = 550$°C for 30 min showed in the first case the high density of fine-scale precipitations with the random distribution (Fig. 31, *a*) and in the second one — the plate-like particles (Fig. 31, *b*).

The high-temperature heat at 775°C, 1 min an alloy aged for 30 min at 400°C transformed fine-scale precipitates or enriched regions of the modulated structure into plate-like particle of the tetragonal α′-phase distributed randomly again (Fig. 31, *c*). Moreover, the plates of the stable β-phase were visible too (Fig. 31, *c*). The similar picture was observed after a reversion at 775°C, 1 min an alloy pre-liminary aged at 550°C for 30 min (Fig. 31, *d*). In this case the small volume fraction of α′-phase was looked too. At that point, its parti-cles lined up forming short rows (Fig. 31, *d*). An analysis of these microstructures showed that after reversion treatment the coarse distribution of the large plate-like particles of incoherent metastable α′ and stable β precipitates has appeared. This corresponded to the loss of the age-hardening effect (Fig. 29).

The comparing of the hardness reversion effect with the results of X-ray and TEM study permits to make the following conclusions.
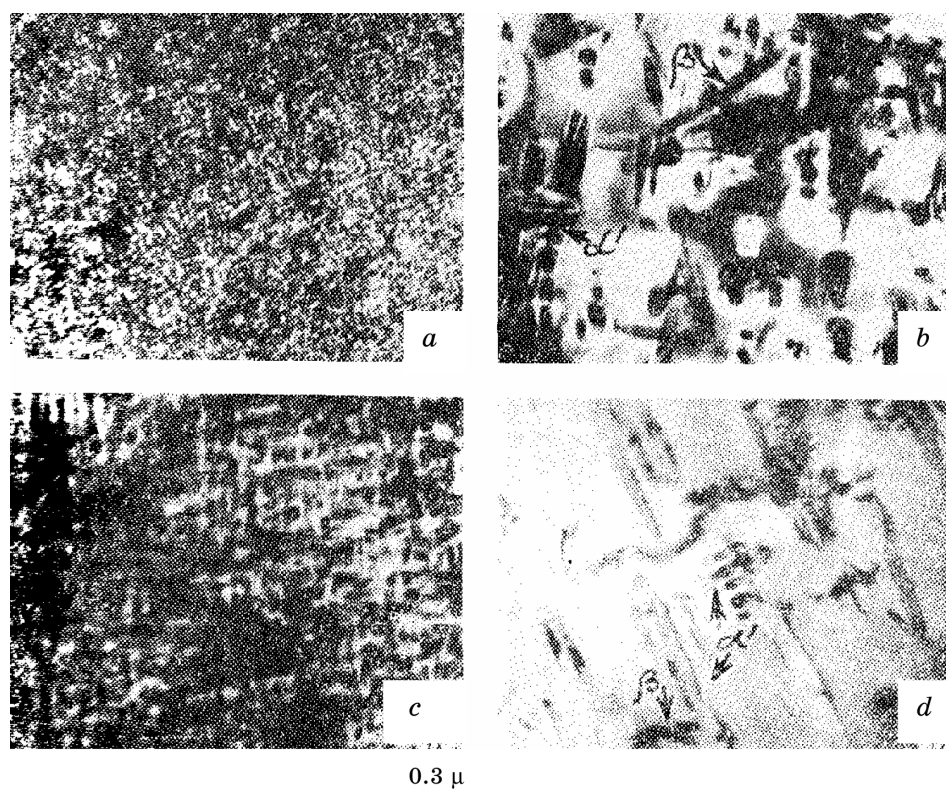
0.3 μ

Fig. 31. Electron microstructures of the Cu–5 at.% Ti alloy after heat-treatments: a — 400°C, 30 min; b — 400°C, 30 min + 775°C, 1 min: c — 550°C, 30 min; d — 550°C, 30 min + 775°C, 1 min. Bright — field [85].

An effect of the reversion depends on; (i) an alloy structure arising after prior aging; (ii) a difference between T_r and T_a: the bigger the reversion effect more. For example, the hardness reversion in alloy with modulation structure (satellite reflexes exist) usually was small or was absent in general. In the literature this question was discussed in terms of a critical particle size or a position of a solvus line for the metastable phase [40]. However, in [86] earnestly showed that the reversion effect was concerned directly with the transitional stage of coalescence too, peculiar for properties that were determined by the distribution function and the relation between the kinetics of particles growth and dissolve at the reversion temperature.

Usually, the transition stage of coalescence is characterized by the α'-phase presence. According to Fig. 2, b the hand-picked reversion
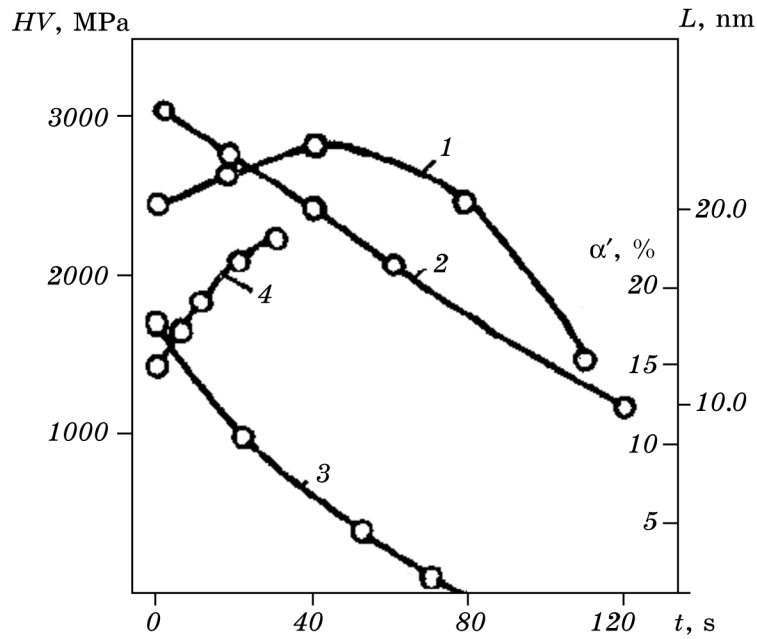
1042 K. V. Chuistov

Fig. 32. Change of the hardness (*1*, *2*), α' — phase particles size (*4*) and relative quantity of α' — phase (*3*) depending on the heating time at 775°C of the Cu−5 at.% Ti alloy aged preliminary at temperatures: *1, 4* — 400°C, 30 min; *2, 3* — 550°C, 30 min [85].

TABLE 8. The dependence of the hardness, a change of the resistivity, a size of the enriched part of M.S. and a phase state of Cu−5 at.% Ti alloy on the aging regime [85].

Heat-treatment	HV, MPa	$\Delta\rho/\rho$, %	Size of enriched part of M.S. (α'-phase), nm	Phase state
400°C, 30 min	2000	18.0	6.0	$\alpha + $ MS
400°, 10 h	2500	25.0	35.0	$\alpha + \alpha'$
500°, 10 h	2450	70.0	100.0	$\alpha + \alpha' + \beta$
550°, 30 min	2250	50.0	30.0	$\alpha + \alpha' + \beta$
550°, 5 h	1930	–	–	$\alpha + \beta$

temperature $T_r = 775°C$ is some greater than the solvus for α'-phase. Therefore it is possible that in such case the nature of the reversion is explained namely by that reason. However, an exist of the rever-

sion effect after heat-treatment 400°C, 10 h + 600°C, 4 min where reversion temperature less than the solvus one pointed to some other cause. Hence, the reversion of the hardness in Cu–Ti alloys is multiform phenomenon and the most likely it occurs due to α'-phase particles dissolve (Fig. 32) or its possible transition to the stable β-phase. The results of the phase analysis were listed in Fig. 32. The different reversion effect in Cu–Ti alloy preaged at various temperatures was explained by the following [79]. If the preaged heat-treatment was 400°C, 30 min the matrix concentration in micro-regions did not get the equilibrium one else $c_m < c_{eq}$. This assuming was supported by data of a resistivity change at 400°C (Table 8). Table. 8 shows that the value $\Delta\rho/\rho$ stops to change only after aging at 500°C, 10 h. On the other words, a matrix composition was far from equilibrium one after early stage of precipitation. On the contrary, after the preaging at 500°C, 10 h (550°C, 30 min) a matrix concentration is near to equilibrium and corresponds to a solvus line of α'-phase (Fig. 2, a). At the reversion temperature T_r a matrix runs up to the concentration c_r and $c_r > c_m > c_{\alpha'}$. Therefore, a degree of the dissolution of structures formed at 400°C will be greater than formed at 500°C, 10 h or at 550°C, 30 min for obtaining by a matrix the same concentration at T_r i.e. $c_r - c_{\alpha'} > c_r - c_m$. This explains the different reversion effect at T_r depending on the preaging regime of Cu–Ti alloy. However, on the other hand, the value of the coherent elastic stresses on the m.s. stage is smaller than in the case of the coherent metastable α'-phase because — off the larger size of particles in the second case (10 nm at 400°C, 30 min and 30–35 nm at 400°C, 10 h). Consequently, the rate of the diffusion through the interface in this case has to bigger due to larger value of coherent stresses [87]. Moreover, partly or full loss of α'-phase coherency during preaging at 500°C, 10 h or 550°C, 30 min stimulates the interface dislocations appearance that may facilitate the $\alpha' > \beta$ phase transition. These argumentations illustrate those fact why the reversion effect is greater on the stage of metastable α'-phase precipitation.

9. Conclusions

1. Age-hardening Cu–Ti alloys correspond to the class of the aging solid solutions where the modulated structure forms on the early stage of the decomposition. At that, such structure is created bit by bit as a result of the coalescence of the coherent particles of the metastable Cu_4Ti ordered phase starting from random distribution of homogeneously nucleated complexes enriched with Ti or fine-scale α'-precipitates. Therefore, the spinodal decomposition proposed in these alloys may be prejudiced. Moreover, up to date the information having a single meaning about the quenched state structure is

absent. As regards the nature of heterogeneities being created during these alloys quenching the analysis of the diffuse scattering distribution in the reciprocal space showed that more acceptable model was the three-dimensional complex — a cell of the three-dimensional modulated structure.

2. The structure of the metastable α'-phase (Cu_4Ti) is tetragonal and non-isomorphic to a matrix although it may be largely coherent that initiates the presence of the additional diffuse scattering along $\langle 110 \rangle$ of a matrix in the X-ray films.

3. The morphology of the metastable α'-phase precipitation is characterized by the transition from random distribution of coherent nucleus to regular one — modulated structure that arises due to elastic interaction between coherent precipitates. The sable β-phase morphology is peculiar two modes: cellular and Widmanstätten form organization.

4. The kinetics of the continuous precipitation of the metastable α'-phase obey the law corresponding to such type of the transformation. The discontinuous precipitation of the stable β-phase is non-monotone: at the beginning of the transformation the value of the cells formation rate increase rapidly then culminates and whereupon quickly go down that is in good comparison with Cahn's theory for boundary precipitation. At the same time, during aging at $550-650°C$ in the Cu–5.7 at.% Ti alloy the volume diffusion plays the definite role in the discontinuous precipitation.

5. An alloying of Cu–Ti solid solutions with the additional element Ag, Be, Cr, Fe, Zr in small quantities (about 1 at.%) causes the change of α'-phase lattice constants and correspondently the values of the misfit. This leads to the different rate of α'-phase particles coarsening. Along with that, an addition of 1, 2, 3 and 5 wt.% Al to Cu–2.3 wt.% Ti alloy causes a suppression of the discontinuous precipitation especially for more alloyed material. Moreover, in Cu–2 at.% Ti with big content of Be (3–6 at.%) the modulated structure and metastable α'-phase formation do not observe but only stable structures CuBe and Cu_3Ti were looked during aging.

6. The plastic deformation of the aging Cu–Ti alloys exerts small influence on the rate of the modulated structure evolution but can produce considerable structural change in the aged and deformed alloy; it destroyes of the modulated structure and contributes to the transition of the metastable α'-phase into stable β-phase. Furthermore, the plastic deformation enlarges essentially the rate of the cellular precipitation due to the acceleration both the cell nucleation and the reaction front mobility.

7. An effect of the ultra-sonic deformation (USD) on age-hardening response of the Cu–Ti alloy depends on the preliminary structure of the aged alloy, on the USD power and on the treatment tem-

perature. The maximal USD effect was found in an alloy aged under USD at aging temperature and containing the modulated structure or the coherent metastable phase particularly. In such case the alloy strengthening relates both due to interaction of the larger density of dislocations with coherent particles and grain-boundary strengthening. Ultra-sonic irradiation at the room temperature of the quenched Cu−Ti alloy provokes only small coarsening of the modulated structures that leads to a little hardening. More strengthening effect of USD is observed on the stage of coherent metastable phase precipitation when the sum of the internal coherent strains and strains from USD exceeded the yield point of the aged alloy.

8. The uniform high pressure reduces the solubility of Ti in Cu and in this way shifts the onset of the cellular precipitation to small time at a definite temperature. On the other hand, the overpressure reduces the rate of the front cell displacement but with a temperature rise this effect become smaller. This effect of pressure on the rate of cellular decomposition is explained by essentially decreasing of the diffusive mobility of Ti atoms on the grain boundaries. At the same time, a reconstruction of the grain boundary during development of the cellular decomposition plays a big role in this process. The overpressure retards such transformation and in that way reduces the cellular decomposition velocity in general.

9. The radioactive irradiation by electrons and neutrons of Cu−Ti aging alloys retards appreciably the cellular decomposition, at that, this effect rises with increasing of irradiation dose. At that point, the neutrons irradiation does not change the relation between the nucleation and growth rates of the cells. The main reason of this effect is that both neutrons and electrons irradiation brake the migration of the front of the cellular decomposition.

10. Aged Cu−Ti alloys have the big age-hardening response due to modulated structure formation. However, in this case the noticeable promotion of the yield stress without alteration of the strengthening coefficient takes place. The main cause of such strengthening effect is the interaction of the dislocations with elastic fields of coherent stresses and with ordered structure of the metastable precipitate when they cut its particles. This phenomenon accompanies by strong localization of the shears in the slip bands. At the same time, the mechanical twining appearance and the transition to more fine slip corresponds to maximal strengthening effect in aged Cu−Ti alloys. *Comparing of the mechanical and processing behavior of Cu−Ti and Cu−Be alloys may conclude that Cu−Ti alloys can replace the beryllium bronze successfully taking into account it bad ecology effect too.*

11. A reversion phenomenon observed in aged Cu−Ti alloy may be many-sided phenomenon. So, an effect of the hardness reversion

depends on: an alloy structure arising after prior aging; a difference between T_r and T_a: the bigger the reversion effect more. Moreover, it often observed if the preliminary aging has corresponded to the transition stage of coalescence or if $T_r > T_s$, where T_s was the solvus temperature for the metastable α'-phase. Additionally, it is necessary to point out that a reversion of the hardness may be total or partial depending on T_r and T_a relation. At last, $\alpha' > \beta$ phase transition occurred at the reversion temperature will be promote the hardness reversion.

REFERENCES

1. J. Pastuhova and A. Rachshtadt, *Pruginnie splavi medi* (Spring copper alloys) (Moscow: Metallurgy: 1979) (in Russian).
2. W. A. Soffa and D. E. Laughlin, *Prog. Mater. Sci.*, 2004 (in press).
3. W. Z. Kroll, *Z. Metallkd.*, **23**: 33 (1931).
4. E. E. Shumacher and W.C. Ellis, *Metals Alloys* **2**: 111 (1931).
5. F. R. Hensel and E. I. Larsen, *Trans. AIME*, **99**: 55 (1932).
6. N. Karllsson, *J. Inst. Metals*, 79: 391 (1951).
7. E. G. Nesterenko and K. V. Chuistov, *Ukr. Fiz. Zh.* 3: 276 (1958) (in Russian).
8. J. Manenc, *Acta Metall.*, **7**: 807 (1959).
9. E. G. Nesterenko and K. V. Chuistov, *Fiz. Met. Metalloved.*, **9**: 140 (1960) (in Russian).
10. C. Bückle and J. Manenc, *J. Mem. Sci. Rev. Metal.*, **57**: 435 (1960).
11. V. Daniel and H. Lipson, *Proc. R. Soc. London A*, **52**: 80 (1940).
12. J. Manemc, *C. R. Acad. Sci.*, **250**: 1814 (1959).
13. E. Y. Nesterenko and K. V. Chuistov, *Kristallogr.*, **10**: 325 (1965) (in Russian).
14. V. V. Kokorin and K. V. Chuistov, *Ukr. Fiz. Zh.*, **13**: 1461 (1968) (in Russian).
15. V. V. Kokorin and K. V. Chuistov, *Fiz. Met. Metalloved.*, **27**: 804 (1969) (in Russian).
16. Yu. D. Tiapkin, *Ann. Rev. Mater. Sci.*, **7**: 209 (1977).
17. T. Tsujimoto, K. Hashimoto, and K. Saito, *Acta Metall.*, **35**: 295 (1977).
18. A. Guinier, *Acta Metall.*, **3**: 510 (1955).
19. O. E. Tkachenko and K. V. Chuistov, *Fiz. Met. Metalloved.*, **29**: 834 (1970) (in Russian).
20. L. P. Gunko, V. V. Kokorin, and K. V. Chuistov, *Fiz. Met. Metalloved.*, **33**: 106 (1973) (in Russian).
21. E. Y. Nesterenko and K. V. Chuistov, *Fiz. Met. Metalloved.*, **9**: 415 (1960) (in Russian).
22. U. Heubner, G. Wassermann, *Z. Metallkd.*, **53**: 152 (1962) (in German).
23. T. Hakkarainen, *Doctoral Thesis*, (Helsenki Univ. of Techn.: Helsenki: 1971).
24. D. E. Laughlin and J. W. Cahn, *Acta Metall.*, **23**: 329 (1975).
25. K. Saito, K. Iida, and R. Watanabe, *Trans. Nat. Res. Inst. Metals*, **9**: 267 (1967).
26. R. C. Ecob, J. V. Bee, and B. Ralph, *Phys. Status Solidi a*, **52**: 201 (1979).
27. J. P Zhang, H. Q. Ye, K. H. Kuo, and S. Amelinks, *Phys. Status Solidi A*,

88: 475 (1985).

28. L. S. Bushnev, A. D. Korotaev, and A. T. Protasov, *Fiz. Met. Metalloved.*, **30:** 63 (1968) (in Russian).
29. K. V. Chuistov, *Metallofiz.*, **41:** 55 (1972) (in Russian).
30. H. T. Michels, I. B. Cadoff, and E. Levine, *Metall. Trans.*, **3:** 667 (1972).
31. J. A. Cornie, A. Datta, and W. A. Soffa, *Metall. Trans.*, **4:** 727 (1973).
32. D. E. Laughlin and J. W. Cahn, *Acta Metall.*, **23:** 329 (1975).
33. A. Datta and W. A. Soffa, *Acta Metall.*, **24:** 987 (1976).
34. V. V. Kokorin, *Fiz. Met. Metalloved.*, **33:** 247 (1972) (in Russian).
35. A. J. Ardell, R. B. Nicholson, and J. D. Eshelby, *Acta Metall.*, **14:** 1295 (1966).
36. A. Nagarajan and P. A. Flin, *Appl. Phys. Lett.*, **11:** 120 (1957).
37. T. Saito and A. Kanio, *Trans. Jap. Inst. Met.*, **31:** 25 (1990).
38. K. V. Chuistov. *Uporyadochenie i raspad.peresishenich tverdich rastvorov* (Ordering and Decomposition of the Super Saturated Solid Solutions) (Kiev: RIO IMP; 1999) (in Russian).
39. N. N. Gangula, V. V. Kokorin, and K. V. Chuistov, *Fiz. Met. Metalloved.*, **33:** 247 (1972) (in Russian).
40. K. V. Chuistov, *Starenie metallicheskih. Splavov* (An Aging of Metallic Alloys) (Kiev: Academperiodika, 2003) (in Russian).
41. M. A Krivoglaz, *Diffuse Scattering of X-Rays and Neutrons by Fluctuations* (Sprinnger: 1994).
42. N. J. Karlson, *J. Inst. Metals.*, **79:** 391 (1951).
43. K. V. Chuistov, *Modulirovanie structuri v stareyuschih splavah* (Modulated Structures in Aging Alloys) (Kiev: Nauk. Dumka: 1975) (in Russian).
44. Yu. D. Tiapkin, I. V. Gongadze, and E. I. Malienko, *Fiz. Met. Metalloved.* **66:** 589 (1988) (in Russian).
45. A. G. Khachaturyan, *Theory of structure transformations in solids* (New York: John Willey & Sons: 1983).
46. Y. Enomoto and K. Kawasaki, *Acta Metal.*, **37:** 1399 (1989).
47. E. I. Malienko and Yu. D. Tiapkin, *Fiz. Met. Metalloved.*, **57:** 942 (1984) (in Russian).
48. A. D. Korotaev, O. V. Tcinenko, and A. T. Protasov, *Fiz. Met. Metalloved.*, **26:** 789 (1968) (in Russian).
49. A. D. Korotaev, A. T. Protasov, O. V. Tcinenko, and O. O. Lambakahar, *Izv. Vissh. Ucheb. Zaved. Fiz.*, No. 9: 113 (1968) (in Russian).
50. J. W. Christian, *Theory of transformations in metals and alloys* (New York: Pergamon Press: 1967).
51. I. M. Lifshits and V. V. Slyozov, *J. Phys. Chem. Solids*, **19:** 35 (1961).
52. T. Doi, *Acta Metal.*, **7:** 291 (1959).
53. D. Turnbull, *Acta Metal.*, **3:** 55 (1955).
54. M. Itkin and O. Smatko, *Dokl. Akad. Nauk UkSSR.*, No. 7: 66 (1980) (in Russian).
55. M. Itkin and O. Smatko, *Metallofiz.*, **4,** No. 4: 118 (1982). (in Russian).
56. M. Itkin and O. Smatko *Dokl. Akad. Nauk UkSSR.*, No. 10: 54 (1984) (in Russian).
57. M. Itkin, V. Krasilnikov, and O. Smatko, *Metallofizi.*, **7,** No. 6: 26 (1985) (in Russian).
58. U. Zwicker, *Z. Metallkd.*, **53:** 706 (1963).

59. J.W. Cahn, *Acta Metal.*, **4**: 449 (1956).
60. L. N. Larikov and O. A. Shmatko, *Yacheisty raspad peresischennih tverdih rastvorov* (The Cellular Decomposition of Super Saturated Solid Solutions) (Kiev: Nauk. dumka: 1976) (in Russian).
61. M. V. Itkin, O. A. Shmatko, and I. G. Primak, *Metallofiz.*, **9**, No. 1: 25 (1987) (in Russian).
62. E. G. Nestrenko and K. V. Chuistov, *Fiz. Met. Metalloved.*, **12**: 567 (1961) (in Russian).
63. A. D. Korotaev, A. T. Protasov, O. V. Tcinenko, and M. V. Lubchenko, *Fiz. Met. Metalloved.*, **27**: 127 (1969) (in Russian).
64. V. N. Vigdorovich and M. V. Malcev, *Izv. Vissh. Ucheb. Zaved. Fiz.*, No. 2: 142 (1958) (in Russian).
65. W. Cruhl and H. Cordier, *Metall.*, **11**: 928 (1957).
66. E. G. Nesterenko and K. V. Chuistov. *Vopr. Fiz. Met. Metalloved.*, No. 13: 142 (1961) (in Russian).
67. R. Knights and P. Wilkes, *Acta Metal.*, **21**: 1503 (1973).
68. E. G. Nesterenko and K. V. Chuistov, *Fiz. Met. Metalloved.*, **12**: 756 (1961) (in Russian).
69. E. G. Nesterenko and K. V. Chuistov, *Vopr. Fiz. Met. Metalloved.*, No. 15: 90 (1962) (in Russian).
70. M. V. Itkin, *Kinetika Yacheistogo Raspada v Splavakh Med — Titan I Vliyanie Razlichnikh Vozdeystviy na ee Parametri* (The Kinetics of the Cellular Decomposition in Copper–Titanium Alloys and The Effect of the Influences on its Parameters (Thesis of Disser for Ph.D.) (Kyyiv: Inst. of Metal Physics: 1986) (in Russian).
71. G. Bazeluk, L. N. Trofimova, and K. V. Chuistov, *Vliyanie ultrazvukovoy deformatcii na fazovie i stukturnie izmeneniya v ctareyuchith splavach* (*Effect of Ultrasonic Deformation on Phase and Structural Transformations I Aging Alloys*) (Kyyiv: 1979) (Prepr./ N.A.S. of the Ukraine, Inst. for Metal Physics, No. 7, 1997) (in Russian).
72. G. Bazeluk, A. L. Beresina, I. G. Polockiy, and K. V. Chuistov, *Ukr. Fiz. Zh.,* **22**: 541 (1977) (in Russian).
73. G. Bazeluk, A. L. Beresina, I. G. Polockiy, and K. V. Chuistov, *Fiz. I Khim. Obrab. Mater.*, No. 3: 116 (1979) (in Russian).
74. G. Stanjck, G. Hornbogen, *Scr. Metal.* **7**: 615 (1973).
75. V. F. Belostotsky and I. G. Polockiy, *Metallofiz.*, **63**: 81 (1976) (in Russian).
76. O. B. Abramov, S. S. Gorelik, and V. P. Grabchak, *Fiz. Tverd. Tela,* **10**: 2514 (1968) (in Russian).
77. G. A. Hayes and I. C. Shyne. *Metal. Sci. J.*, **2**:81.(1968).
78. A. Shinyaev, *Fazovie prevrascheniya i svoystva splavov pri visokith davleniyath* (Phase transformations and Alloys properties at High Pressures) (Moscow: Nauka: 1973) (in Russian).
79. M. V. Itkin, I. A. Osipenko., T. V. Shirina, and O. A. Shmatko, *Fiz. Met. Metalloved.*, **65**: 1027 (1988) (in Russian).
80. R. Wirtl and H. Gleiter, *Acta Metal.*, **29**: 1829 (1981).
81. M. V. Itkin, Yu. V. Kornushin, and O. A. Shmatko, *Fiz. Met. Metalloved.*, **68**: 772 (1989) (in Russian).
82. A. D. Korotaev, O. O. Lambakahar, and A. T. Protasov, *Fiz. Met. Metalloved.*, **27**: 645 (1969) (in Russian).

83. K. P. Kalinin and M. Z. Spiridonova, *Tcvetn. Met.* (Moscow), No1:82 (1959) (in Russian).
84. R. R. Romanova, A. N. Uksusnikov, and Yu. M. Ustugov, *Fiz. Met. Metalloved.*, **78**: 5 (1994) (in Russian).
85. A. L. Beresina and K. V. Chuistov, *Metallofiz.*, **49**: 72 (1973) (in Russian).
86. A. L. Beresina and K. V. Chuistov, *Fiz. Met. Metalloved.*, **50**: 333 (1980) (in Russian).
87. H. K. Cook and J. E. Hilliard, *J. Appl. Phys.*, **40**: 2191 (1969).